Natural strain variation reveals diverse biofilm regulation in squid-colonizing *Vibrio fischeri*

Ella R. Rotman[1,†], Katherine M. Bultman[2,†], John F. Brooks II[1,4], Mattias C. Gyllborg[1], Hector L. Burgos[2], Michael S. Wollenberg[3], Mark J. Mandel[1,2,*]

[1] Department of Microbiology-Immunology, Northwestern University Feinberg School of Medicine, Chicago, IL USA

[2] Department of Medical Microbiology and Immunology, University of Wisconsin-Madison, Madison, WI USA

[3] Department of Biology, Kalamazoo College, Kalamazoo, MI USA

[4] Current address: Department of Immunology, The University of Texas Southwestern Medical Center, Dallas, TX USA

[†] Authors contributed equally

Short title: *Vibrio fischeri* biofilm regulatory evolution

Keywords: Biofilm, phosphorelay, RscS, BinK, Vibrio fischeri, Aliivibrio fischeri

* Correspondence to:

Mark J. Mandel
University of Wisconsin-Madison
Department of Medical Microbiology and Immunology
1550 Linden Drive
Madison, WI 53706
Phone: (608) 261-1170
Fax: (608) 262-8418
Email: mmandel@wisc.edu

ABSTRACT

The mutualistic symbiont *Vibrio fischeri* builds a symbiotic biofilm during colonization of squid hosts. Regulation of the exopolysaccharide component, termed Syp, has been examined in strain ES114, where production is controlled by a phosphorelay that includes the inner membrane hybrid histidine kinase RscS. Most strains that lack RscS or encode divergent RscS proteins cannot colonize a squid host unless RscS from a squid symbiont is heterologously expressed. In this study, we examine *V. fischeri* isolates worldwide to understand the landscape of biofilm regulation during beneficial colonization. We provide a detailed study of three distinct evolutionary groups of *V. fischeri* and find that while the RscS-Syp biofilm pathway is required in one of the groups, two other groups of squid symbionts require Syp independent of RscS. Mediterranean squid symbionts, including *V. fischeri* SR5, colonize without an RscS homolog encoded in their genome. Additionally, Group A *V. fischeri* strains, which form a tightly-related clade of Hawaii isolates, have a frameshift in *rscS* and do not require the gene for squid colonization or competitive fitness. These same strains have a frameshift in *sypE*, and we provide evidence that this Group A *sypE* allele leads to an upregulation in biofilm activity. This work thus describes the central importance of Syp biofilm in colonization of diverse isolates, and demonstrates that significant evolutionary transitions correspond to regulatory changes in the *syp* pathway.

IMPORTANCE

Biofilms are surface-associated, matrix-encased bacterial aggregates that exhibit enhanced protection to antimicrobial agents. Previous work has established the importance of biofilm formation by a strain of luminous *Vibrio fischeri* bacteria as the bacteria colonize their host, the Hawaiian bobtail squid. In this study, expansion of this work to many natural isolates revealed

that biofilm genes are universally required, yet there has been a shuffling of the regulators of those genes. This work provides evidence that even when bacterial behaviors are conserved, dynamic regulation of those behaviors can underlie evolution of the host colonization phenotype. Furthermore, this work emphasizes the importance of investigating natural diversity as we seek to understand molecular mechanisms in bacteria.

INTRODUCTION

A fundamental question in studying host-associated bacterial communities is understanding how specific microbial taxa assemble reproducibly in their host. Key insights into these processes were first obtained by studying plant-associated microbes, and the discovery and characterization of Nod factors in Rhizobia was valuable to understand how partner choice between microbe and host could be mediated at the molecular level (1, 2). There are complex communities in humans and other vertebrate animals, yet metagenomic and imaging analyses of these communities have revealed striking reproducibility in the taxa present and in the spatial arrangement of those taxa (3–5). Invertebrate animal microbiomes provide appealing systems in which to study microbiome assembly in an animal host: the number of taxa are relatively small, and examination and manipulation of these organisms have yielded abundant information about processes underlying host colonization (6). For this work we focused on the binary symbiosis between *Vibrio fischeri* and bobtail squids, including the Hawaiian bobtail squid, *Euprymna scolopes*. Bobtail squid have an organ for the symbiont termed the light organ, and passage of specific molecules between the newly-hatched host and the symbiont leads to light organ colonization specifically by planktonic *V. fischeri* and not by other bacteria (7–9). The colonization process involves initiation, accommodation, and persistence steps, resulting in light organ crypt colonization by *V. fischeri*. Upon colonization of the squid light organ, bacteria accumulate to high density and produce light. The bacterial light is modulated by the host to

camouflage the moonlight shadow produced by the nighttime foraging squid in a cloaking process termed counter-illumination (10, 11). A diel rhythm leads to a daily clearing of 90-95% of the bacteria from the crypts and regrowth of the remaining cells (12). However, the initial colonization process, including biofilm-based aggregation on the host ciliated appendages, occurs only in newly-hatched squid. This work examines regulation of biofilm formation in diverse squid-colonizing *V. fischeri* strains.

In the well-studied *V. fischeri* strain ES114, biofilm formation is required to gain entry into the squid host. RscS is a hybrid histidine kinase that regulates *V. fischeri* biofilm formation through a phosphorelay involving the hybrid histidine kinase SypF and the response regulator and σ^{54}-dependent activator SypG (13–15). This pathway regulates transcription of the symbiosis polysaccharide (Syp) locus, which encodes regulatory proteins (SypA, SypE, SypF, and SypG), glycosyltransferases, factors involved in polysaccharide export, and other biofilm-associated factors (14, 16). The products of the ES114 *syp* locus direct synthesis and export of a biofilm exopolysaccharide that is critical for colonization. Additional pathways have been identified to influence biofilm regulation in ES114, including the SypE-SypA pathway and inhibition of biofilm formation by BinK and HahK (17–21).

V. fischeri biofilm regulation is connected to host colonization specificity. In the Pacific Ocean, the presence of *rscS* DNA is strongly correlated to the ability to colonize squid (22). As one example, while the fish symbiont MJ11 encodes a complete *syp* locus, it lacks RscS and does not robustly colonize squid. Heterologous expression of ES114 RscS in MJ11 activates the biofilm pathway and is sufficient to enable squid colonization (22). Similarly, addition of ES114 RscS to *mjapo*.8.1--a fish symbiont that encodes a divergent RscS that is not functional for squid colonization--allows the strain to colonize squid (22). RscS has also been shown to be necessary for squid colonization in certain strains. In addition to ES114, interruption of *rscS* in

V. fischeri strains KB1A97 and MJ12 renders them unable to colonize squid. Previous phylogenetic analysis revealed that ancestral *V. fischeri* do not encode *rscS*, and that it was acquired once during the organism's evolution, likely allowing for an expansion in host range. From this analysis, it was concluded that strains with *rscS* can colonize squid, with the only exception being the fish symbionts that harbor the divergent RscS, including *mjapo*.8.1 (22).

There are similar *Vibrio*-squid associations worldwide, yet only *V. fischeri* and the closely-related *Vibrio logei* have been isolated from light organs (23–26). Our 2009 study revealed that although most symbionts have *rscS* DNA, there are Mediterranean *V. fischeri* (e.g., SR5) that do not have *rscS* yet can colonize squid (22, 24, 27). This unexpected finding prompted the current work to examine whether strains such as SR5 colonize with the known biofilm pathway or with a novel pathway. Here, we show that all *V. fischeri* strains tested require the *syp* locus to colonize a squid host, and we identify two groups of isolates that colonize with novel regulation. Given the exquisite specificity by which *V. fischeri* bacteria colonize squid hosts, this work reinforces the importance of biofilm formation and reveals different regulatory modes across the evolutionary tree.

RESULTS

Most *V. fischeri* strains synthesize biofilm in response to RscS overexpression. Biofilm formation is required for squid colonization, and overexpression of the biofilm regulator RscS in strain ES114 stimulates a colony biofilm on agar plates (15). Our previous work demonstrated that *V. fischeri* strain MJ11 synthesizes a colony biofilm under similar inducing conditions, which is notable because MJ11 does not encode RscS in its chromosome (22). While the ancestral strain MJ11 did not encode RscS, it had what seemed to be an intact *syp* locus, and overexpression of the heterologous RscS from ES114 was sufficient to enable robust squid

147 colonization (22). We examined a phylogenetic tree of *V. fischeri* isolates (Fig. 1), and in this
148 study we expand our analysis of RscS-Syp biofilm regulation in a wider group of *V. fischeri*
149 strains.
150
151 Initially, we asked whether responsiveness to RscS overexpression would yield a similar colony
152 biofilm in this diverse group of strains. We took the same approach as our previous study and
153 introduced plasmid pKG11, which overexpressed ES114 RscS, into strains across the
154 evolutionary tree (22, 28). We observed that almost all strains tested, including those that lack
155 *rscS*, were responsive to overexpression of ES114 RscS (Fig. 2). The morphology of the colony
156 biofilms differed across isolates; but in most cases colony biofilm was evident at 24 h and
157 prominent at 48 h. All of the strains exhibited some wrinkled colony morphology at 48 h with the
158 exception of CG101, which was isolated from the pineapplefish *Cleidopus gloriamaris (25)*.
159 These results demonstrated that most *V. fischeri* strains can produce biofilm in response to
160 RscS overexpression, and this includes strains that presumably have not encountered *rscS* in
161 their evolutionary history.
162
163 One unexpected observation was that there was a subset of *rscS*-encoding strains that were
164 reproducibly delayed in their colony biofilm, and had only a mild wrinkled colony phenotype at
165 48 h (strains MB11B1, ES213, KB2B1; Fig. 2). We considered whether this was due to
166 differential growth of the strains, but resuspension of spots and dilution plating to determine
167 CFU/spot demonstrated no significant growth difference between these strains and ES114
168 under these conditions. The strains are closely-related (Fig. 1) and a previous study had noted
169 that this group shared a number of phenotypic characteristics, e.g. reduced motility in soft agar
170 (29). Those authors termed this tight clade as “Group A” *V. fischeri* (30). Our results in Figure 2
171 argue that Group A strains do not respond to RscS in the same manner as other *V. fischeri*
172 strains, which prompted us to investigate the evolution of the RscS-Syp signaling pathway. We

have maintained the Group A nomenclature here, and furthermore we introduce the nomenclature of Group B (a paraphyletic group of strains that contain *rscS*; this group includes the common ancestor of all *rscS*-containing strains) and Group C (a paraphyletic group of strains that contains the common ancestor of all *V. fischeri* - these strains do not contain *rscS*), as shown in Figure 1.

Ancestral Group C squid isolates colonize *E. scolopes* independent of RscS and dependent on Syp. Group C strains generally cannot colonize squid, yet there are Mediterranean squid isolates that appear in this group (Fig. 1; (22)). The best-studied of these strains, SR5, was isolated from *Sepiola robusta*, is highly luminous, and colonizes the Hawaiian bobtail squid *E. scolopes* (24). Nonetheless, this strain lacks *rscS* (27). We first asked whether the strain can colonize in our laboratory conditions, and we confirmed that it colonizes robustly, consistent with the result result previously published by Fidopiastis et al. (24) (Fig. 3). Next, we asked whether it uses the Syp biofilm to colonize. To address this question, we deleted the 18 kb *syp* locus (i.e., *sypA* through *sypR*) in strains SR5 and ES114. Deletion of *rscS* or the *syp* locus in ES114 led to a substantial defect in colonization, consistent with a known role for these factors (Fig. 3). Similarly, deletion of the *syp* locus in SR5, a strain that does not encode *rscS*, led to a dramatic reduction in colonization (Fig. 3). Therefore, even though strain SR5 does not encode *rscS*, it can colonize squid, and it requires the *syp* locus to colonize normally.

RscS is dispensable for colonization in Group A strains. We noted in the wrinkled colony biofilm assays shown in Figure 2 that Group A strains exhibited a more modest response to overexpression of RscS. Sequencing of the native *rscS* gene in these strains revealed a predicted -1 frameshift (ΔA1141) between the PAS domain and the histidine kinase CA domain. Whereas ES114 and other Group B strains have nine adenines at this position, the Group A strains have eight, leading to a frameshift and then truncation at an amber stop codon, raising

the possibility that Group A strains have a divergent biofilm signaling pathway (Fig. 4A). Given the importance of RscS in the Group B strains including ES114, we considered the possibility that this apparent frameshift encoded a functional protein, either through ribosomal frameshifting or through the production of two polypeptides that together provided RscS function; there is precedent for both of these concepts in the literature (31, 32). We first introduced a comparable frameshift into a plasmid-borne overexpression allele of ES114 *rscS*, and this allele did not function with the deletion of the single adenine (Fig. 4B). This result suggested to us that the frameshift in the Group A strains may not be functional. Therefore, we proceeded to delete *rscS* in two Group A strains (MB11B1, ES213) and two Group B strains (ES114, MB15A4). The Group B strains required RscS for squid colonization (Fig. 5A). However, the Group A strains exhibited no deficit in the absence of *rscS* (Fig. 5A). We next attempted a more sensitive assay in which a Group A strain was competed against MB15A4. Previous studies have demonstrated that in many cases Group A strains outcompete Group B strains (30, 33). We competed Group A strain MB11B1 against Group B strain MB15A4 and observed a significant competitive advantage for the Group A strain, as was observed previously (30). Deletion of *rscS* in the Group A strain did not affect competitive fitness, demonstrating that MB11B1 can outcompete a Group B strain even if MB11B1 lacks RscS (Fig. 5B).

The *syp* locus is broadly required for squid colonization. Given that Group A strains seemed to represent a tight phylogenetic group in which RscS was not required for colonization or competitive fitness, we next asked whether this group requires the Syp biofilm for colonization. We proceeded to delete the entire *syp* locus in two Group A and two Group B strains and to conduct single-strain colonization analysis. In each strain assayed, the *syp* locus was required for full colonization, and we observed a 2-4 log reduction in CFU per animal in the absence of the *syp* genes, pointing to a critical role for Syp biofilm in these strains (Fig. 6). In

Group A strains in particular, no colonization was detected in the absence of the *syp* locus. Additionally, we isolated a transposon insertion in SR5 *sypJ*, and this strain did not colonize squid well, arguing that this effect is due to the Syp biofilm and not due to regulation of a distinct phenotype by regulators within the locus.

Group A strains encode an alternate allele of SypE. It seemed curious to us that Group A strains do not encode a functional RscS and do not require *rscS* for colonization, yet in many cases Group A strains can outcompete Group B strains (e.g. MB11B1 in Fig. 5B; and Refs. (30, 33)). We reasoned that if the Syp biofilm had a different regulatory architecture in Group A strains--e.g., constitutively activated or activated by a different regulatory protein--then this could explain the Syp regulation independent of RscS. Genome sequencing of SR5 and MB11B1 did not identify a unique histidine kinase that was likely to directly substitute for RscS (27, 33). Given that the *syp* locus encodes biofilm regulatory proteins, we examined *syp* conservation. We used TBLASTN with the ES114 Syp proteins as queries to determine amino acid conservation in the other *V. fischeri* Group A strain MB11B1, Group C strain SR5, and the *Vibrio vulnificus* type strain ATCC 27562 (34, 35). As shown in Figure 7, ES114 SypE, a response regulator and serine kinase/phosphatase that is a negative regulator of the Syp biofilm (17, 36), exhibited the lowest level of conservation among *syp* locus products. *V. vulnificus* does not encode a SypE ortholog (37), as the syntenic (but not homologous) RbdE encodes a predicted ABC transporter substrate-binding protein. The closest hit for SypE was AOT11_RS12130 (9% identity), compared to 7% identity for the RbdE. Due to the reduced conservation at both the strain and species levels, we analyzed *V. fischeri* MB11B1 SypE in greater detail. Examination of the *sypE* coding sequence revealed an apparent -1 frameshift mutation in which the position 33 (guanine in ES114 and adenine in other Group B and C strains examined) is absent in Group A strains (Fig. 7B). We therefore considered the hypothesis that SypE is nonfunctional in Group

A, and that these strains can colonize because they are lacking a functional copy of this negative regulator that is itself regulated by RscS.

To test this hypothesis, we relied on knowledge of the biofilm regulatory pathway from ES114, in which overexpression of SypG produces a wrinkled colony phenotype, but only in strains lacking SypE activity (38, 39). Therefore, we introduced the SypG-overexpressing plasmid pEAH73 into strains as a measure of whether the SypE pathway was intact. In the ES114 strain background, we observed cohesive wrinkled colony formation at 48 h in an ES114 Δ*sypE* strain, but not in the wild-type parent (Fig. 8A). If the *sypE* frameshift observed in MB11B1 led to a loss of function, then introduction of that frameshift into ES114 would lead to a strain that is equivalent to the Δ*sypE* strain. We constructed this strain and upon SypG overexpression we observed wrinkled colony formation. Surprisingly, the biofilm phenotype was observed earlier (i.e., by 24 h) and leads to more defined colony biofilm architecture at 48 h. While the lack of SypE leads to increased and more rapid biofilm formation, in this assay we observed an even greater increase as a result of the frameshift in *sypE* (Fig. 8A).

We proceeded to conduct a similar assay in the MB11B1 strain background. The colony biofilm phenotypes were muted compared to the ES114 background, but the pattern observed is the same. Strains lacking the additional nucleotide at position 33 (i.e., the native MB11B1 allele) exhibited the strongest cohesion, whereas strains with the nucleotide to mimic ES114 *sypE* (i.e., added back in MB11B1 *sypE*(nt::33G)) were not cohesive (Fig. 8B). These results argue that a novel allele of *sypE* is found in Group A strains and this allele results in more substantial biofilm formation than in a Δ*sypE* strain.

Our finding that the MB11B1 *sypE* allele promotes biofilm formation bolstered the model that this allele contributes to the ability of MB11B1 to colonize squid independent of RscS. To test

this model, we introduced the frameshift into ES114 or "corrected" the frameshift in MB11B1. We then conducted single-strain colonization assays, and in each case the *sypE* allele alone was not sufficient to alter the overall colonization behavior of the strain (Fig. 9). Therefore, these data suggest that the frameshift in the MB11B1 *sypE* is not sufficient to explain its ability to colonize independent of RscS, and therefore other regions of SypE and/or other loci in the MB11B1 genome contribute to its ability to colonize independent of RscS.

BinK is active in Group A, B, and C strains. We recently described the histidine kinase, BinK, which negatively regulates *syp* transcription and Syp biofilm formation (18). In ES114, overexpression of BinK impairs the ability of *V. fischeri* to colonize. We therefore reasoned that if BinK could function in Group A strains and acted similarly to repress Syp biofilm, then overexpression of BinK would reduce colonization of these strains. We introduced the pBinK plasmid (i.e., ES114 *binK* (18)) and asked whether multicopy *binK* would affect colonization. In strain MB11B1, BinK overexpression led to a dramatic reduction in colonization (Fig. 10A). Therefore, there is a clear effect for BinK overexpression on the colonization of the Group A strain MB11B1.

We attempted to ask the same question in Group C strain SR5, but the pES213-origin plasmids were not retained during squid colonization. Therefore, we instead asked whether deletion of the BinK, a negative regulator of ES114 colonization, has a comparable effect in SR5 (18). We deleted *binK* and observed a 2.4-fold competitive advantage during squid competition (Fig. 10B), arguing that BinK in this Group C strain is active and performs an inhibitory function similar to that in ES114.

We next examined the colony biofilm phenotype for strains lacking BinK. MB11B1 Δ*binK* exhibited a mild colony biofilm phenotype at 48 h, as evidenced by the cohesiveness of the spot

when disrupted with a toothpick (Fig. 10C). The colonies also exhibited an opaque phenotype. In a minority of experimental replicates, wrinkled colony morphology was evident at 48 h, but in all samples wrinkled colony morphology was visible at 7 d (data not shown). The SR5 Δ*binK* strain also exhibited slightly elevated biofilm morphology at 48 h, though the cells were not as cohesive as those of MB11B1 Δ*binK* (Fig. 10C). Together, the results in Figure 10 argue that BinK, a factor that has been characterized as a negative regulator of Syp biofilm, plays similar roles in Group A and Group C strains and has a widely-conserved function across the *V. fischeri* evolutionary tree.

DISCUSSION

This study examines regulation of a beneficial biofilm that is critical to host colonization specificity in *V. fischeri.* The Syp biofilm was discovered thirteen years ago and has been characterized extensively for its role in facilitating squid colonization by *V. fischeri.* This work establishes that the *syp* locus is required broadly across squid symbionts, and it uncovers three groups of *V. fischeri* that use different regulatory programs upstream of the *syp* locus. A simplified phylogenetic tree showing key features of squid symbionts in these three groups is shown in Figure 11.

There are three nested evolutionary groups of *V. fischeri* that have been described separately in the literature and here we formalize the nomenclature of Groups C, B, and A. Group A is a monophyletic group, as are Groups AB and ABC (Fig. 1). This work provides evidence that squid symbionts in each group have a distinct biofilm regulatory architecture. Most *V. fischeri* isolates that have been examined from the ancestral Group C cannot colonize squid; however, those that can colonize do so without the canonical biofilm regulator RscS. We show that the known targets of RscS regulation—genes in the *syp* biofilm locus—are nonetheless required for

328 squid colonization by this group. Group B strains include the well-characterized ES114 strain,
329 which requires RscS and the *syp* locus to colonize squid. Group A strains differ phenotypically
330 and behaviorally from the sister Group B strains (30), and we demonstrate that these strains
331 have altered biofilm regulation. Group A strains have a frameshift in *rscS* that renders it
332 nonfunctional, and a 1 bp deletion in *sypE*, and we provide evidence that the *sypE* allele
333 promotes biofilm development in the absence of RscS. Additionally, we note that the *sypE*
334 frameshift is not present in SR5, arguing for distinct modes of biofilm regulation in Groups A, B,
335 and C.
336
337 At the same time, this study provides evidence that some aspects of biofilm regulation are
338 conserved in diverse squid symbionts, such as the effects of the strong biofilm negative
339 regulator BinK. Published data indicate that evolved BinK alleles can alter colonization of H905
340 (Group B) and MJ11 (Group C), and that a deletion of MJ11 *binK* leads to enhanced
341 colonization (20). Our experiments in Figure 10 show a clear effect for BinK in all three
342 phylogenetic groups. We also observed responsiveness to RscS overexpression in all squid
343 symbionts examined (Fig. 2). CG101 was the only *V. fischeri* strain examined that did not exhibit
344 a colony biofilm in response to RscS overexpression. CG101 was isolated from the Australian
345 fish *Cleidopus gloriamaris*; based on these findings, we suspect that the strain does not have an
346 intact *syp* locus or otherwise has divergent biofilm regulation.
347
348 It remains a formal possibility that the entire *syp* locus is not required in Group A or Group C,
349 but instead that only one or a subset of genes in the locus are needed. We have constructed
350 Campbell-type (insertion duplication) alleles to interrupt *sypG* in MB11B1 and SR5, and
351 additionally have isolated a transposon insertion in SR5 *sypJ*, and none were able to colonize
352 well. Additionally, aggregation in squid mucus has been observed for the Group A strain
353 MB13B2, and this aggregation is dependent on *sypQ* (40). In our data we note that Group A

strains were completely unable to colonize in the absence of the *syp* locus, unlike the tested Group B & C strains that exhibited reduced colonization in their respective mutants (Figs. 3, 6). Therefore, the simplest explanation is that the *syp* locus is required in divergent strains in a manner similar to how it is used in ES114. We think that the ability to completely delete the *syp* locus is a clean way to ask whether the locus is required for specific phenotypes, and our strains are likely to be useful tools in probing Syp protein function in diverse *V. fischeri* isolates.

It is intriguing to speculate as to how the two frameshifts in the Group A strains arose, and why the nonfunctional RscS is tolerated in this group. One possible scenario is that the Group A strains acquired a new regulatory input into the Syp pathway, and that the presence of this new regulator bypassed the requirement for RscS. We note that comparative genomic analysis of Hawaiian D (dominant)-type strains--which largely overlap with Group A--revealed an additional 250 kb of genomic DNA compared to other isolates, yielding a large cache of genes that could play a role in this pathway (33). A related possibility is that *rscS*-independent colonization results from altered regulation of the *syp* locus, either due to changes in regulators (e.g. SypF) or sites that are conserved with Group B. An additional possibility is that the *sypE* frameshift arose, enabling Group A strains to colonize independent of *rscS*. Given that correction of this frameshift in MB11B1 does not significantly affect colonization ability (Fig. 9), this sequence of events seems less likely, and we expect that another regulator in MB11B1 is required for the RscS-independent colonization phenotype. There is evidence that under some conditions LuxU can regulate the *syp* biofilm (41), and as this protein is conserved in *V. fischeri* it may play an important role in Group A or Group C.

Results from two experimental conditions suggest that the Group A strains may have an elevated baseline level of biofilm formation. Our data indicate that in the absence of BinK or upon SypG overexpression, MB11B1 colonies exhibit strong cohesion under conditions in which

ES114 does not (Figs. 8, 10). Furthermore, we note that the Group A strain MB11B1, when lacking BinK, also exhibits a darker, or more opaque, colony phenotype (Fig. 10). This phenotype has been observed in some ES114 mutants (16) but not in the corresponding ES114 Δ*binK* strain (Fig. 10). The entire colonization lifecycle likely requires a balance between biofilm formation/cohesion and biofilm dispersal, and these data argue that Group A strains may be more strongly tilted toward the biofilm-producing state. There is evidence that strains lacking BinK exhibit a colonization advantage in the laboratory (18, 20), suggesting that this strategy of more readily forming biofilms may provide a fitness advantage in nature. At the same time, the biofilm negative regulator BinK is conserved among *V. fischeri* strains examined (including MB11B1; Fig. 10), arguing that there is a benefit to reducing biofilm formation under some conditions.

Our study provides hints as to the role of SypE in MB11B1 and other Group A strains. In ES114, the C-terminus is a PP2C serine kinase domain, whereas the N-terminus of SypE is an RsbW serine phosphatase domain. SypE acts to phosphorylate and dephosphorylate SypA Ser-56, with the unphosphorylated SypA being the active form to promote biofilm development (17). The balance between SypE kinase and phosphatase is modulated by a central two-component receiver domain (17). Our data that the MB11B1 *sypE* allele promotes biofilm formation suggest that the protein is tilted toward the phosphatase activity. In MB11B1, the frameshift early in *sypE* suggests that there is a different start codon and therefore a later start codon. An alternate GTG start codon in MB11B1 occurs corresponding to codon 18 in ES114 *sypE* (Fig. 7), and this is likely the earliest start for the MB11B1 polypeptide. We attempted to directly identify the SypE N-terminus by mass spectrometry, yet we could not identify the protein from either strain. Additional study is required to elucidate how MB11B1 SypE acts to promote biofilm formation.

V. fischeri strains are valuable symbionts in which to probe the molecular basis to host colonization specificity in animals (22, 25, 26). A paradigm has emerged in which biofilm formation through the RscS-Syp pathway is required for squid colonization but not for fish colonization. This study affirms a role of the Syp biofilm, but at the same time points out divergent (RscS-independent) regulation in Group C and Group A isolates. In another well-studied example of symbiotic specificity, Rhizobial Nod factors are key to generating specificity with the plant host, yet strains have been identified that do not use this canonical pathway (42, 43). Future work will elaborate on these RscS-independent pathways to determine how non-canonical squid colonization occurs in diverse natural isolates.

MATERIALS & METHODS

Bacterial strains and growth conditions. *V. fischeri* and *E. coli* strains used in this study can be found in Table 1. *E. coli* strains, used for cloning and conjugation, were grown in Luria-Bertani (LB) medium (25 g Difco LB Broth [BD] per liter). *V. fischeri* strains were grown in Luria-Bertani salt (LBS) medium (25 g Difco LB Broth [BD], 10 g NaCl, and 50 ml 1 M Tris buffer pH 7.0, per liter). Growth media were solidified by adding 15 g Bacto agar (BD) per liter. When necessary, antibiotics (Gold Biotechnology) were added at the following concentrations: tetracycline, 5 µg/ml for *V. fischeri*; erythromycin, 5 µg/ml for *V. fischeri*; kanamycin, 50 µg/ml for *E. coli* and 100 µg/ml for *V. fischeri*; and chloramphenicol, 25 µg/ml for *E. coli*, 2.5 -5 µg/ml for Group B *V. fischeri*, and 1 - 2.5 µg/ml for Group A *V. fischeri*. The two MB11B1 / pKV69 strains listed reflect two separate constructions of this strain, though we have not identified any differences between them.

Phylogenetic analysis. Phylogenetic reconstructions assuming a tree-like topology were created with three methods: maximum parsimony (MP); maximum likelihood (ML); and

Bayesian inference (Bayes) as previously described (22, 30). Briefly, MP reconstructions were performed by treating gaps as missing, searching heuristically using random addition, tree-bisection reconnection with a maximum of 8 for swaps, and swapping on best only with 1000 repetitions. For ML and Bayesian analyses, likelihood scores of 1500+ potential evolutionary models were evaluated using both the corrected and uncorrected Akaike Information Criterion, the Bayesian Information Criterion, and Decision Theory (Performance Based Selection) as implemented by jModelTest2.1 (44). For all information criteria, the most optimal evolutionary model was a symmetric model with a proportion of invariable sites and a gamma distribution of rate heterogeneity (SYM+I+Γ).

ML reconstruction was implemented via PAUP*4.0a163 (45) by treating gaps as missing, searching heuristically using random addition, tree-bisection reconnection for swaps, and swapping on best only with 1000 repetitions. Bayesian inference was done by invoking the 'nst=6' and 'rates=invgamma' and 'statefreqpr=fixed(equal)' settings in the software package MrBayes3.2.6 (46). The Metropolis-coupled Markov chain Monte Carlo (MCMCMC) algorithm used to estimate the posterior probability distribution for the sequences was set up with 'temp=0.2' and one incrementally 'heated' chain with three 'cold' chains; these four chains were replicated two times per analysis to establish convergence of the Markov chains (i.e., 'stationarity' as defined by (47) and interpreted previously in (30)). For this work, stationarity was achieved after approximately 50,000 samples (5,000,000 generations) were collected, with 25% discarded. The ~37,500 samples included were used to construct a 50% majority-rule consensus tree from the sample distribution generated by MCMCMC and assess clades' posterior probabilities. For ML and MP analyses, the statistical confidence in the topology of each reconstruction was assessed using 1000 bootstrap replicates. Phylogenetic trees were visualized with FigTree 1.4.3 (http://tree.bio.ed.ac.uk/software/figtree); the final tree was edited for publication with Inkscape 0.91 (http://inkscape.org/) and GIMP 2.8.22 (http://www.gimp.org/).

457

458 **DNA synthesis and sequencing.** Each of the primers listed in Table 3 was synthesized by
459 Integrated DNA Technologies (Coralville, IA). Full inserts from all cloned constructs were
460 verified by Sanger DNA sequencing through ACGT, Inc via the Northwestern University
461 Feinberg School of Medicine NUSeq Core Facility; or the University of Wisconsin-Madison
462 Biotechnology Center. Sequence data was analyzed with SeqMan Pro (DNAStar software),
463 SnapGene (GSL Biotech), and Benchling.

464

465 **Construction of gene deletions.** Deletions in *V. fischeri* strains ES114 and MB11B1 were
466 made according to the lab's gene deletion protocol: doi:10.5281/zenodo.1470836. In brief, 1.6
467 kb upstream and 1.6 kb downstream of the targeted gene or locus were cloned into linearized
468 plasmid pEVS79 (amplified with primers pEVS79_rev_690/pEVS79_for_691) using Gibson
469 Assembly (NEBuilder HiFi DNA Assembly cloning kit) with the primer combinations listed in
470 Table S1. The Gibson mix, linking together the upstream and downstream flanking regions, was
471 transformed into *E. coli* on plates containing X-gal, with several white colonies selected for
472 further screening by PCR using primers flanking the upstream/downstream junction (Tables 3
473 and S1). The resulting plasmid candidate was confirmed by sequencing and conjugated into the
474 *V. fischeri* recipient by tri-parental mating with helper plasmid pEVS104, selecting for the
475 chloramphenicol resistance of the plasmid backbone. *V. fischeri* colonies were first screened for
476 single recombination into the chromosome by maintaining antibiotic resistance in the absence of
477 selection and then screened for double recombination by the loss of both the antibiotic resistant
478 cassette and the gene/locus of interest. Constructs were verified by PCR (Table 3) and
479 sequencing.

480

481 Deletion of SR5 *binK* was conducted using Splicing by Overlap Extension PCR (SOE-PCR) and
482 natural transformation (method modified from (48)). Oligos binK-F1 and binK-R1-LUH, and

483 oligos binK-F2-RUH and binK-R2 were used in a PCR with MJM1125 (SR5) genomic DNA as
484 the template to amplify DNA fragments containing ~1 kb of sequence upstream and
485 downstream relative to *binK*, respectively. Using SOE-PCR, these fragments were fused on
486 either side to a third DNA fragment containing an Erm^R cassette, which was amplified using
487 pHB1 as template and oligos HB41 and HB42. We then used natural transformation with
488 pLostfoX (49) to insert this mutagenic DNA into MJM1125, where the flanking sequences guide
489 the Erm^R cassette to replace *binK*, generating the desired gene deletion. Candidate SR5 Δ*binK*
490 mutants were selected after growth on LBS-Erm5 plates. Oligos binK-F1 and binK-R2, and HB8
491 and binK-FO were used to screen candidates for the correct deletion scar by PCR, and oligos
492 KMB_036 and KMB_037 were used to confirm the absence of *binK* in the genome. The deletion
493 was verified by Sanger sequencing with primers HB8, HB9, HB42, and HB146. The base
494 plasmid pHB1 contains an erythromycin resistance cassette flanked by FRT sites, and was
495 constructed using oligos HB23 and HB39 with gBlock gHB1 (sequence in Supplementary File
496 S1; Integrated DNA Technologies, Inc.) as template to amplify the Erm^R cassette flanked by
497 HindIII and BamHI sites, which was then cloned into the corresponding site in pUC19.
498
499 For most constructs, the deleted genetic material was between the start codon and last six
500 amino acids (50), with two exceptions: the Δ*sypE* in MJM1130 included the ATG that is two
501 amino acids upstream of the predicted start codon, but not the canonical start codon; and the
502 Δ*binK* alleles in MJM1117, MJM1130, and MJM2114, which were constructed to be equivalent
503 to MJM2251 (Δ*binK* in ES114) (18). The Δ*binK* alleles in these strains include the start codon,
504 the next six codons, two codons resulting from ATCGAT (ClaI site), and the last three codons
505 for a predicted 12 amino acid peptide.
506
507 **Construction of *sypE* alleles.** To create *sypE*(ntG33Δ) in MJM1100 and *sypE*(nt33::G) in
508 MJM1130, the single point mutation was created by amplifying the gene in two halves, with the

509 N-terminal portion consisting of approximately 300 bp upstream of *sypE* up through nucleotide
510 33 and the C-terminal portion consisting of nucleotide 33 and the remaining *sypE* gene. The
511 overlap between the two halves contained the single nucleotide polymorphism in the primers
512 that connected them. The altered *sypE* alleles were initially cloned into plasmid pEVS107
513 (linearized with primers pEVS107_3837/pEVS107_3838) using Gibson Assembly and then the
514 entire altered *sypE* allele was subcloned into pEVS79 with Gibson Assembly (Table S1). After
515 double recombination of the vector into *V. fischeri*, candidate colonies for the altered *sypE* in
516 MJM1100 were screened with primers ES114_indel_for/ES114_indel_rev. The primer set
517 anneals more strongly to the wildtype *sypE* sequence than to *sypE*(ntG33::Δ). Candidates in the
518 MJM1100 background with a fainter PCR band were sequenced and confirmed to have the
519 *sypE*(ntG33::Δ) allele. For MJM1130, the primer set MB11B1_indel_for/MB11B1_indel_rev
520 anneals more strongly to the *sypE*(nt33::G) allele than to the naturally occurring *sypE* allele and
521 candidates in MJM1130 that contained a more robust PCR band were selected for sequencing
522 to be confirmed as being *sypE*(nt33::G).
523
524 **Construction of pKG11 *rscS1*(ntA1141::Δ)**. Plasmid pKG11 encodes an overexpression allele
525 of RscS, termed *rscS1 (15, 28)*. *rscS* nucleotide A1141 was deleted on the plasmid using the
526 Stratagene Quikchange II Site-Directed Mutagenesis Kit with primers rscS_del1F and
527 rscS_del1R. The resulting plasmid, pMJM33, was sequenced with primers MJM-154F and
528 MJM-306R to confirm the single base pair deletion.
529
530 **Squid colonization**. Hatchling *E. scolopes* were colonized by exposure to approximately 3 x
531 10^3 CFU/ml (ranging from 5.2 x 10^2 - 1.4 x 10^4 CFU/ml; as specified in figure legends) of each
532 strain in a total volume of 40 ml of FSIO (filter-sterilized Instant Ocean) for 3 hours. Squid were
533 then transferred to 100 ml of FSIO to stop the inoculation and then transferred to 40 ml FSIO for
534 an additional 45 hours with a water change at 24 hours post inoculation. For Figure 10A,

kanamycin was added to the FSIO to keep selective pressure on the plasmid. After 48 hours of colonization, the squid were euthanized and surface sterilized by storage at -80 ºC, according to standard practices (51). For determination of CFU per light organ, hatchlings were thawed, homogenized, and 50 µl of homogenate dilutions was plated onto LBS plates. Bacterial colonies from each plate were counted and recorded. Mock treated, uncolonized hatchlings ("apo-symbiotic") were used to determine the limit of detection in the assay. The competitive index (CI) was calculated from the relative CFU of each sample in the output (light organ) versus the input (inoculum) as follows:

Log_{10} ((Test strain[light organ] / Control strain[light organ]) / (Test strain[inoculum] / Control strain[inoculum])). For competitions of natural isolates, the Group A strain (or its Δ*rscS* derivative) was the test strain and the Group B strain was the control strain. Colony color was used to enumerate colonies from each--white for Group A strains MB11B1 and ES213; yellow for Group B strains ES114 and MB15A4--along with PCR verification of selected colonies. For competition between SR5 and SR5 Δ*binK*, 100 colonies per squid were patched onto LBS-Erm5 and LBS.

Colony biofilm assays. Bacterial strains were grown in LBS media (Fig. 10C) or LBS-Cam2.5 media (Figs. 2, 8) for approximately 17 hours, then 10 µl (Fig. 2) or 8 µl (Fig. 8, 10C) was spotted onto LBS plates (Fig. 10C) or LBS-Tet5 plates (Figs. 2, 8). Spots were allowed to dry and the plates incubated at 25 °C for 48 hours. Images of the spots were taken at 24 and 48 h post-spotting using a Leica M60 microscope and Leica DFC295 camera. After 48 h of growth, the spots were disrupted using a flat toothpick and imaged similarly.

Analysis of DNA and protein sequences *in silico*. Amino acid sequences for *V. fischeri* ES114 *syp* genes were obtained from RefSeq accession NC_006841.2. Local TBLASTN queries were performed for each protein against nucleotide databases for the following strains,

each of which were derived from the RefSeq cds_from_genomic.fna file: *V. fischeri* SR5 (GCA_000241785.1), *V. fischeri* MB11B1 (GCA_001640385.1) and *V. vulnificus* ATCC27562 (GCA_002224265.1). Percent amino acid identity was calculated as the identity in the BLAST query divided by the length of the amino acid sequence in ES114. Domain information is from the PFAM database (52).

FIGURE LEGENDS

Figure 1. *Vibrio fischeri* phylogeny, highlighting the source of each strain. Bayesian phylogram (50% majority-rule consensus) inferred with a SYM+I+Γ model of evolution for the concatenated gene fragments *recA*, *mdh*, and *katA*. In this reconstruction, the root connected to a clade containing the four non-*V. fischeri* outgroup taxa. Statistical support is represented at nodes by the following three numbers: upper left, Bayesian posterior probability (of approximately 37,500 non-discarded samples) multiplied by 100; upper right, percentage of 1000 bootstrap Maximum Likelihood pseudo-replicates; bottom middle center, percentage of 1000 bootstrap Maximum Parsimony pseudo-replicates. Statistical support values are listed only at nodes where more than 2 methods generated support values ≥ 50%. Strains sharing identical sequences for a given locus fragment are listed next to a vertical bar at a leaf; because of a lack of space, some support values have been listed either immediately to the right of their associated nodes and are marked with italicized lower-case Roman numerals in the phylogram. The isolation habitat and geography of each strain are indicated by symbol and color, respectively. The black bar represents 0.01 substitutions/site.

Figure 2. Most *V. fischeri* strains tested form colony biofilm in response to RscS overexpression. Spot assays of the indicated *V. fischeri* strains carrying pKV69 (vector) or pKG11 (*rscS1*; overexpressing ES114 *rscS*) after 24 and 48 h. Strains are MJM1268, MJM1269, MJM1246, MJM1247, MJM1266, MJM1267, MJM1219, MJM1221, MJM1238,

MJM1239, MJM1104, MJM1106, MJM1276, MJM1277, MJM1270, MJM1271, MJM1258, MJM1259, MJM1254, MJM1255, MJM1242, MJM1243, MJM1240, MJM1241, MJM1272, MJM1273, MJM1274, MJM1275, MJM1278, MJM1279, MJM1109, MJM1111, MJM1280, MJM1281, MJM1260, MJM1261, MJM1244, MJM1245, MJM1256, and MJM1257. Different phenotypes were observed in the isolates examined; in most cases we observed wrinkled colonies, but in some cases we observed only a subtle pocked pattern (EM30), and in other cases we did not observe any change in colony morphology compared to the vector control (noted by *). The black bar is 5 mm in length.

Figure 3. Squid colonization in Group C strain SR5, which does not encode RscS, is dependent on the *syp* polysaccharide locus. Single-strain colonization experiments were conducted and circles represent individual animals. The limit of detection for this assay, represented by the dashed line, is 7 CFU/LO, and the horizontal bars represent the median of each set. Hatchling squid were inoculated with 1.5-3.2 × 10^3 CFU/ml bacteria, washed at 3 h and 24 h, and assayed at 48 h. Each dot represents an individual squid. Strains are: MJM1100, MJM3010, MJM3062, MJM1125, and MJM3501. Statistical comparisons by the Mann-Whitney test, ** $p<0.01$, *** $p<0.001$, **** $p<0.0001$.

Figure 4. Group A strains have a frameshift in *rscS*. (A) ES114 RscS protein domains. Nucleotides 1114-1173 in ES114 RscS (AF319618) and their homologous sequences in the other Group B and Group A strains are listed. The -1 frameshift is present in the Group A *rscS* alleles. The ES114 reading frame is noted on the top of the alignment and the Group A reading frame on the bottom, which is predicted to end at the amber stop codon. (B) Deletion of nucleotide A1141 in ES114 to mimic this frameshift in pKG11 renders it unable to induce a colony biofilm in a spot assay at 48 h. Strains are MJM1104, MJM1106, and MJM2226.

Figure 5. Group A strains MB11B1 and ES213 do not require RscS for squid colonization. Wild-type (WT) and Δ*rscS* derivatives of the indicated strains were assayed in (A) a single-strain colonization assay and (B) competitive colonization against Group B strain MB15A4. Hatchling squid were inoculated at 3.5-14 × 10^3 CFU/ml bacteria, washed at 3 h and 24 h, and assayed at 48 h. Each dot represents an individual squid. (A) Strains: MJM1100, MJM3010, MJM2114, MJM3042, MJM1130, MJM3046, MJM1117, and MJM3017. The limit of detection is represented by the dashed line, and the horizontal bars represent the median of each set. In both panels, open dots are wild type and filled dots are Δ*rscS*. (B) The competitive index (CI) is defined in the methods and is shown on a Log_{10} scale. Strains: MJM1130 and MJM3046, each competed against MJM2114. Values greater than 1 indicate more MB11B1. Statistical comparisons by the Mann-Whitney test, ns not significant, **** p<0.0001.

Figure 6. Group B and Group A strains require the *syp* locus for robust squid colonization. Wild type (WT) and Δ*syp* derivatives of the indicated strains were assayed in a single strain colonization assay. Hatchling squid were inoculated with 6.7-32 × 10^2 CFU/ml bacteria (ES114 and MB15A4 backgrounds) or 5.2-8.9 × 10^2 CFU/ml bacteria (MB11B1 and ES213 backgrounds), washed at 3 h and 24 h, and assayed at 48 h. Each dot represents an individual squid. The limit of detection is represented by the dashed line and the horizontal bars represent the median of each set. Strains are MJM1100, MJM3062, MJM2114, MJM3071, MJM1130, MJM3065, MJM1117, and MJM3068. Statistical comparisons by the Mann-Whitney test, **** p<0.0001.

Figure 7. Group A strains have a frameshift in *sypE*. (A) Amino acid identity in the Syp locus. Results show the identity from TBLASTN query using the *V. fischeri* ES114 protein sequences as queries against genes in the homologous loci in *V. fischeri* strains or *V. vulnificus* ATCC

27562. The identity for SypE against *V. vulnificus* is plotted for the syntenous RbdE, although this is not the highest TBLASTN hit, as described in the text. (B) ES114 SypE protein domains. Nucleotides 1-60 in ES114 *sypE* and their homologous sequences in the other Group C, B, and A strains are listed. A -1 frameshift is present in the Group A *sypE* alleles. The ES114 reading frame is noted on the top of the alignment and the Group A reading frame on the bottom, which is predicted to end at the amber stop codon. A possible GTG start codon for the resumption of translation in the ES114 reading frame is present at the position corresponding to the 18th codon in ES114 *sypE*.

Figure 8. The MB11B1 *sypE* frameshift leads to an enhanced biofilm phenotype upon SypG overexpression. Spot assays of strains carrying the pKV69 vector or pEAH73 SypG overexpression plasmid. (A) ES114 strain background. Strains lacking SypE produce a wrinkled colony phenotype upon SypG overexpression. Deletion of nucleotide 33 in *sypE* to mimic the Group A frameshift led to earlier wrinkling and a more pronounced colony biofilm at 48 h. Strains: MJM1104, MJM3455, MJM3418, MJM3419, MJM3364, and MJM3365. (B) Group A strain MB11B1, which naturally carries a -1 frameshift in *sypE*, exhibits a cohesive phenotype at 48 h with overexpression of SypG. Deletion of *sypE* reduces this phenotype, and repairing the frameshift by addition of a guanosine at nucleotide 33 further reduces the cohesiveness of the spot. Strains: MJM3370, MJM3371, MJM3411, MJM3412, MJM3398, and MJM3399.

Figure 9. The *sypE* -1 frameshift allele is not sufficient to affect colonization ability. The indicated strains were assayed in a single-strain colonization assay. Gray boxes denote alleles distinct from their wild-type background. Frameshift “fs” refers to alleles--relative to an ES114 reference--that lack *rscS* nucleotide A1141, or that lack *sypE* nucleotide G33. The wild-type MB11B1 strain contains natural frameshifts in these loci, and the ES114 nt33::ΔG allele was constructed. Addition back of the nucleotide in MB11B1 *sypE* is denoted as “(+)”. Hatchling

665 squid were inoculated with 6.8-8.4 × 10^2 CFU/ml bacteria (MB11B1 background) or 4.0-5.4 ×
666 10^3 CFU/ml bacteria (ES114 background), washed at 3 h and 24 h, and assayed at 48 h. Each
667 dot represents an individual squid. The limit of detection is represented by the dashed line and
668 the horizontal bars represent the median of each set. Strains are MJM1100, MJM3010,
669 MJM4323, MJM3394, MJM1130, and MJM3397. Statistical comparisons by the Mann-Whitney
670 test, ns not significant.
671
672 **Figure 10. BinK is active in Groups A, B, and C**. (A) Overexpression of pBinK inhibits
673 colonization in Group A strain MB11B1. Hatchling squid were inoculated with 3.6-6.8 × 10^3
674 CFU/ml bacteria, washed at 3 h and 24 h, and assayed at 48 h. Each dot represents an
675 individual squid. The limit of detection is represented by the dashed line and the horizontal bars
676 represent the median of each set. The vector control is pVSV104. Strains are MJM1782,
677 MJM2386, MJM2997, and MJM2998. (B) Deletion of *binK* confers a colonization defect in Group
678 C strain SR5. Strains are MJM1125 and MJM3571; mean inoculum of 7.2 × 10^3 CFU/ml;
679 median competitive index (CI) was 0.38 (i.e., 2.4-fold advantage for the mutant). (C) Deletion of
680 the native *binK* in MB11B1 yielded opaque and cohesive spots, which are stronger phenotypes
681 than we observe in ES114. Strains are MJM1100, MJM2251, MJM1130, MJM3084, MJM2997,
682 and MJM2998. Statistical comparisons by the Mann-Whitney test, **** $p<0.0001$.
683
684 **Figure 11. Summary model of distinct modes of biofilm formation in squid-colonizing *V.***
685 ***fischeri***. Phylogenetic tree is simplified from Figure 1, and illustrates key features of squid
686 symbionts in the three groups. Shown are divergent aspects (RscS, SypE) and conserved
687 regulation (BinK). In all groups, the *syp* exopolysaccharide locus is required for squid
688 colonization.
689
690 **SUPPLEMENTAL FILES**

691

692 **Table S1 (PDF). Primer pairs for construction of the deletion mutants**. Detailed

693 oligonucleotide and construction details for deletions and the MJM1100 sypE(ntG33Δ) and

694 MJM1130 *sypE*(*nt33*::*G*) strains.

695

696 **File S1 (PDF). Sequence of the synthetic dsDNA, gBlock_erm.** The sequence is provided in

697 FASTA format printed as PDF.

698

699

700 **Table 1. Bacterial strains.**

Strain	**Genotype**	**Source/Reference**
V. fischeri		
MJM1059	MJ11	(25, 53)
MJM1100	ES114	(54)
MJM1104	ES114 (MJM1100) / pKV69	This study
MJM1106	ES114 (MJM1100) / pKG11	This study
MJM1109	MJ11 (MJM1059) / pKV69	This study
MJM1111	MJ11 (MJM1059) / pKG11	This study
MJM1114	MJ12	(53)
MJM1115	CG101	(25)

MJM1117	ES213	(55)
MJM1119	EM18	(25, 53)
MJM1120	EM24	(53, 56)
MJM1121	EM30	(53)
MJM1122	WH1	(57)
MJM1125	SR5	(24)
MJM1126	SA1	(24)
MJM1127	KB1A97	(29)
MJM1128	KB2B1	(29)
MJM1129	KB5A1	(29)
MJM1130	MB11B1	(29)
MJM1136	EM17	(56)
MJM1147	*mjapo*.6.1	(22)
MJM1149	*mjapo*.7.1	(22)
MJM1151	*mjapo*.8.1	(22)
MJM1153	*mjapo*.9.1	(22)
MJM1219	*mjapo*.8.1 / pKV69	This study

MJM1221	*mjapo*.8.1 / pKG11	This study
MJM1238	MJ12 (MJM1114) / pKV69	This study
MJM1239	MJ12 (MJM1114) / pKG11	This study
MJM1240	SR5 (MJM1125) / pKV69	This study
MJM1241	SR5 (MJM1125) / pKG11	This study
MJM1242	SA1 (MJM1126) / pKV69	This study
MJM1243	SA1 (MJM1126) / pKG11	This study
MJM1244	MB11B1 (MJM1130) / pKV69	This study
MJM1245	MB11B1 (MJM1130) / pKG11	This study
MJM1246	EM17 (MJM1136) / pKV69	This study
MJM1247	EM17 (MJM1136) / pKG11	This study
MJM1254	KB1A97 (MJM1127) / pKV69	This study
MJM1255	KB1A97 (MJM1127) / pKG11	This study
MJM1256	KB2B1 (MJM1128) / pKV69	This study
MJM1257	KB2B1 (MJM1128) / pKG11	This study
MJM1258	KB5A1 (MJM1129) / pKV69	This study
MJM1259	KB5A1 (MJM1129) / pKG11	This study

MJM1260	ES213 (MJM1117) / pKV69	This study
MJM1261	ES213 (MJM1117) / pKG11	This study
MJM1266	EM18 (MJM1119) / pKV69	This study
MJM1267	EM18 (MJM1119) / pKG11	This study
MJM1268	EM24 (MJM1120) / pKV69	This study
MJM1269	EM24 (MJM1120) / pKG11	This study
MJM1270	EM30 (MJM1121) / pKV69	This study
MJM1271	EM30 (MJM1121) / pKG11	This study
MJM1272	*mjapo*.6.1 (MJM1147) / pKV69	This study
MJM1273	*mjapo*.6.1 (MJM1147) / pKG11	This study
MJM1274	*mjapo*.7.1 (MJM1149) / pKV69	This study
MJM1275	*mjapo*.7.1 (MJM1149) / pKG11	This study
MJM1276	*mjapo*.9.1 (MJM1151) / pKV69	This study
MJM1277	*mjapo*.9.1 (MJM1151) / pKG11	This study
MJM1278	CG101 (MJM1115) / pKV69	This study
MJM1279	CG101 (MJM1115) / pKG11	This study
MJM1280	WH1 (MJM1122) / pKV69	This study

MJM1281	WH1 (MJM1122) / pKG11	This study
MJM1782	ES114 (MJM1100) pVSV104	(18)
MJM2114	MB15A4	(29)
MJM2226	ES114 (MJM1100) / pMJM33	This study
MJM2251	ES114 (MJM1100) Δ*binK*	(18)
MJM2386	ES114 (MJM1100) / pBinK	This study
MJM2997	MB11B1 (MJM1130) / pVSV104	This study
MJM2998	MB11B1 (MJM1130) / pBinK	This study
MJM2999	ES213 (MJM1117) / pVSV104	This study
MJM3000	ES213 (MJM1117) / pBinK	This study
MJM3010	ES114 (MJM1100) Δ*rscS*	This study
MJM3017	ES213 (MJM1117) Δ*rscS*	This study
MJM3042	MB15A4 (MJM2114) Δ*rscS*	This study
MJM3046	MB11B1 (MJM1130) Δ*rscS*	This study
MJM3062	ES114 (MJM1100) Δ*syp*	This study
MJM3065	MB11B1 (MJM1130) Δ*syp*	This study
MJM3068	ES213 (MJM1117) Δ*syp*	This study

MJM3071	MB15A4 (MJM2114) Δ*syp*	This study
MJM3084	MB11B1 (MJM1130) Δ*binK*	This study
MJM3354	ES114 (MJM1100) *sypE*(ntG33Δ)	This study
MJM3364	ES114 (MJM1100) *sypE*(ntG33Δ) / pKV69	This study
MJM3365	ES114 (MJM1100) *sypE*(ntG33Δ) / pEAH73	This study
MJM3370	MB11B1 (MJM1130) / pKV69	This study
MJM3371	MB11B1 (MJM1130) / pEAH73	This study
MJM3394	ES114 (MJM1100) Δ*rscS* *sypE*(ntG33Δ)	This study
MJM3397	MB11B1 (MJM1130) *sypE*(nt33::G)	This study
MJM3398	MB11B1 (MJM1130) *sypE*(nt33::G) / pKV69	This study
MJM3399	MB11B1 (MJM1130) *sypE*(nt33::G) / pEAH73	This study
MJM3410	MB11B1 (MJM1130) Δ*sypE*	This study
MJM3411	MB11B1 (MJM1130) Δ*sypE* / pKV69	This study
MJM3412	MB11B1 (MJM1130) Δ*sypE* / pEAH73	This study
MJM3417	ES114 (MJM1100) Δ*sypE*	This study
MJM3418	ES114 (MJM1100) Δ*sypE* / pKV69	This study
MJM3419	ES114 (MJM1100) Δ*sypE* / pEAH73	This study

MJM3423	ES114 (MJM1100) Δ*rscS* Δ*sypE*	This study
MJM3455	ES114 (MJM1100) / pEAH73	This study
MJM3501	SR5 (MJM1125) Δ*syp*	This study
MJM3751	SR5 (MJM1125) ΔbinK::*erm*	This study
E. coli		
MJM534	CC118 λpir / pEVS104	(58)
MJM537	DH5α λpir	Lab stock
MJM570	DH5α / pEVS79	(58)
MJM580	DH5α λpir / pVSV104	(59)
MJM581	DH5α / pKV69	(60)
MJM583	DH5α / pKG11	(15)
MJM639	XL1-Blue / pMJM33	This study
MJM658	BW23474 / pEVS107	(61)
MJM2384	DH5α λpir / pBinK	(18)
MJM2540	KV5264 / pEAH73	(39)
MJM3008	DH5α / pEVS79-Δ*rscS*[MJM1100]	This study
MJM3014	DH5α λpir / pEVS79-Δ*rscS*[MJM1117]	This study

MJM3039	DH5α λpir / pEVS79-Δ*rscS*[MJM2114]	This study
MJM3043	DH5α λpir / pEVS79-Δ*rscS*[MJM1130]	This study
MJM3060	NEB5α / pEVS79-Δ*syp*[MJM1100]	This study
MJM3063	NEB5α / pEVS79-Δ*syp*[MJM1130]	This study
MJM3066	DH5α λpir / pEVS79-Δ*syp*[MJM1117]	This study
MJM3069	DH5α λpir / pEVS79-Δ*syp*[MJM2114]	This study
MJM3082	NEB5α / pEVS79-Δ*binK*[MJM1130]	This study
MJM3287	NEB5α / pHB1	This study
MJM3338	DH5α λpir / pEVS107-*sypE*[MJM1130](nt33::G)	This study
MJM3340	DH5α λpir / pEVS107-*sypE*[MJM1100](ntG33Δ)	This study
MJM3351	NEB5α / pEVS79-*sypE*[MJM1130](nt33::G)	This study
MJM3352	NEB5α / pEVS79-*sypE*[MJM1100](ntG33Δ)	This study
MJM3409	NEB5α / pEVS79-Δ*sypE*[MJM1130]	This study
MJM3416	NEB5α / pEVS79-Δ*sypE*[MJM1100]	This study

701

702 **Table 2. Plasmids.**

Plasmid	**Relevant genotype**	**Source/Reference**
pEVS79	Vector backbone (Cam^R) for deletion	(58)

	construction	
pKV69	Vector backbone (Cam^R/Tet^R)	(60)
pKG11	pKV69 carrying *rscS1*	(15)
pMJM33	pKG11 *rscS1*(ntA1141::Δ)	This study
pEVS104	Conjugation helper plasmid (Kan^R)	(58)
pEVS107	Mini-Tn7 mobilizable vector (Erm^R/Kan^R)	(61)
pEAH73	pKV69 carrying *sypG* from ES114	(39)
pVSV104	Complementation vector (Kan^R)	(59)
pBinK	pVSV104 carrying *binK* from MJM1100	(18)
pHB1	pUC19 FRT-*erm*-FRT	This study
pEVS79-Δ*rscS*[MJM1100]	pEVS79 carrying 1.6 kb US/1.6 kb DS of *rscS* from MJM1100	This study
pEVS79-Δ*rscS*[MJM1117]	pEVS79 carrying 1.6 kb US/1.6 kb DS of *rscS* from MJM1117	This study
pEVS79-Δ*rscS*[MJM2114]	pEVS79 carrying 1.6 kb US/1.6 kb DS of *rscS* from MJM2114	This study
DH5α λpir / pEVS79-Δ*rscS*[MJM1130]	pEVS79 carrying 1.6 kb US/1.6 kb DS of *rscS* from MJM1130	This study
pEVS79-Δ*syp*[MJM1100]	pEVS79 carrying 1.6 kb US of *sypA*/1.6 kb DS of *sypR* from MJM1100	This study
pEVS79-Δ*syp*[MJM1130]	pEVS79 carrying 1.6 kb US of *sypA*/1.6 kb DS of *sypR* from MJM1130	This study
pEVS79-Δ*syp*[MJM1117]	pEVS79 carrying 1.6 kb US of *sypA*/1.6 kb DS of *sypR* from MJM1117	This study

pEVS79-Δ*syp*[MJM2114]	pEVS79 carrying 1.6 kb US of *sypA*/1.6 kb DS of *sypR* from MJM2114	This study
pEVS79-Δ*binK*[MJM1130]	pEVS79 carrying 1.6 kb US/1.6 kb DS of *binK* from MJM1130	This study
pEVS107-*sypE*[MJM1130](nt33::G)	pEVS107 carrying the *sypE*(nt33::G) allele from MJM1130	This study
pEVS107-*sypE*[MJM1100](ntG33Δ)	pEVS107 carrying the *sypE*(ntG33Δ) allele from MJM1100	This study
pEVS79-*sypE*[MJM1130](nt33::G)	pEVS79 carrying the *sypE*(nt33::G) allele from MJM1130	This study
pEVS79-*sypE*[MJM1100](ntG33Δ)	pEVS79 carrying the *sypE*(ntG33Δ) allele from MJM1100	This study
pEVS79-Δ*sypE*[MJM1130]	pEVS79 carrying 1.6 kb US/1.6 kb DS of *sypE* from MJM1130	This study
pEVS79-Δ*sypE*[MJM1100]	pEVS79 carrying 1.6 kb US/1.6 kb DS of *sypE* from MJM1100	This study

703

704

705 **Table 3. DNA oligonucleotides for PCR amplification and sequencing.**

Primer name	**Sequence (5' to 3')**
DAT_015F	ACCAAGAAGCAGTACGACGATTAT
ES114_DS_ver	GGATGTTTTAGATGTTGCGG
ES114_indel_for	TTACTTTTTTCAGATACAAAGCCC
ES114_indel_rev	GTTGTTCTGATAGTGCGTGA
ES114_US_ver	ATCAACTCAAGAAACTCCCC

for_ver_sypE	CCGGCTCAAACTATTGCAG
Gib_ES114_binK_DS_for	attaatcgatGCGTATACATAAATAATGATTCATATATAC
Gib_ES114_binK_DS_rev	gcaggaattcgatatcaagcTTTCAATACTGTGTTTTTATGC
Gib_ES114_binK_US_for	gaggtcgacggtatcgataaGAGCCTTTTAAATCCCCTAAC
Gib_ES114_binK_US_rev	atgtatacgcATCGATTAATGACATATTATTATTCATAAAAAAC
Gib_ES114_rscS_DS_for	taatgcaatgGAGAAGTATGAAACACAATAAAC
Gib_ES114_rscS_DS_rev	gcaggaattcgatatcaagcAAAAATACATTGTTGCACTTG
Gib_ES114_rscS_US_for	gaggtcgacggtatcgataaGACGTCTAAAACTGAATCG
Gib_ES114_rscS_US_rev	catacttctcCATTGCATTAGCTCCTATAAAATAG
Gib_ES114_syp_DS_for	gcttattatgATATTTGCTCGAGGCCAATAAAAAC
Gib_ES114_syp_DS_rev	gcaggaattcgatatcaagcTGGTGAATGTAGGATCCAC
Gib_ES114_syp_US_for	gaggtcgacggtatcgataaCAACCGTAGCGCCAAATG
Gib_ES114_syp_US_rev	gagcaaatatCATAATAAGCTCCTAGGGAATAATC
Gib_ES114_sypE_C_for	cagatacaaaCCCACATCACTAGAGTCG
Gib_ES114_sypE_C_rev	ctagtggccaggtacctcgaAATTAAGCTTCCATCTTCAC
Gib_ES114_sypE_DS_for	tgtaatcatgCTGTTAATTGAGAATCAATAAAAAG
Gib_ES114_sypE_DS_rev	caactctttttccgaaggtaTTGAGTAACCGGCATAATTTAG

Gib_ES114_sypE_N_for	tagagggccctaggcgcgccTGTTTCACAACTCAATACC
Gib_ES114_sypE_N_rev	gtgatgtgggTTTGTATCTGAAAAAAGTAAAGTAG
Gib_ES114_sypE_US_for	gaggtcgacggtatcgataaTGGTCAGATGAAATGTCATTTTTAG
Gib_ES114_sypE_US_rev	caattaacagCATGATTACACCACTGTTG
Gib_ES213_rscS_US_rev	catacttctcCATTGTATTAGCTCCTATAAAATAG
Gib_MB11B1_syp_DS_for	gcttattatgATATTTGCTCGAGGTCAATAAAAG
Gib_MB11B1_syp_US_for	gaggtcgacggtatcgataaGCACACTGATAACTAAATTATTAC
Gib_MB11B1_syp_US_rev	gagcaaatatCATAATAAGCTCCTAGGG
Gib_MB11B1_sypE_C_for	cagatacaaaGCCAACATCACTAGAATC
Gib_MB11B1_sypE_C_rev	ctagtggccaggtacctcgaTCAACAATTAAGCTTCCATC
Gib_MB11B1_sypE_DS_for	cagtggtatgCTGTTAATTGAAAACCAATAGC
Gib_MB11B1_sypE_DS_rev	gcaggaattcgatatcaagcATTTAGGATGTTTTTAATAACAATTTG
Gib_MB11B1_sypE_N_for	tagagggccctaggcgcgccAGTTTCACAACTCAATACTAATAATATTC
Gib_MB11B1_sypE_N_rev	tgatgttggcTTTGTATCTGAAAAAAGCAAAATAG
Gib_MB11B1_sypE_US_for	gaggtcgacggtatcgataaGAATGGTCAGATGAAATGTC
Gib_MB11B1_sypE_US_rev	caattaacagCATACCACTGTTGATAAAAATC
Gib_pEVS79_ES_sypE_for	gaggtcgacggtatcgataaTGTTTCACAACTCAATACC

Gib_pEVS79_ES_sypE_rev	gcaggaattcgatatcaagcAATTAAGCTTCCATCTTCAC
Gib_pEVS79_MB_sypE_for	gaggtcgacggtatcgataaAGTTTCACAACTCAATACTAATAATATTC
Gib_pEVS79_MB_sypE_rev	gcaggaattcgatatcaagcTCAACAATTAAGCTTCCATC
Gib_SR5_syp_DS_for	gcttattatgATATTTGCTCGAGGACAATAAAAAG
Gib_SR5_syp_DS_rev	gcaggaattcgatatcaagcTGGTGAGTGTAGAATCCATTC
Gib_SR5_syp_US_for	gaggtcgacggtatcgataaAACCGTAGCGCCAAATGG
Gib_SR5_syp_US_rev	gagcaaatatCATAATAAGCTCCTAGGGAATAATCC
HB8	ACAAAATTTTAAGATACTGCACTATCAACACACTCTTAAG
HB9	GGGAGGAAATAATCTAGAATGCGAGAGTAGG
HB23	TTGGAGAGCCAGCTGCGTTCGCTAA
HB39	TAGGAAGCTTACGAGACGAGCTTCTTATATATGCTTCGCCAGGAAGTTCCTATTCTCTAGAAAGTATAGGAACTTCCTTAGAAGCAAACTTAAGAGTGTG
HB41	CGATCTTGTGGGTAGAGACATCCAGGTCAAGTCCAGCCCCGCTCTAGTTTGGGAATCAAGTGCATGAGCGCTGAAG
HB42	ACGAGACGAGCTTCTTATATATGCTTCGCCAG
HB146	CGATCTTGTGGGTAGAGACATC
binK-F1	GAAATTACCATGGAGCCAACAGCAAGAC
binK-R1-LUH	ctggcgaagcatatataagaagctcgtctcgtCATAAAAAACCTAGCGCTTTATTTGTAGATATAATTATTAACTATAATCGC

binK-F2-RUH	gacttgacctggatgtctctacccacaagatcgCGCTCATTGTATCTATAGAGTATGTACTGAGTTACG
binK-R2	GGCATCATTATGGCAACCATTAAAGACG
binK-FO	CCGTTAATACTGGATTATTCGCTTGAATTTGAACG
KMB_036	CCACAATAGCAGAATACAAATTCGCTG
KMB_037	CTCAAAATGACAGTCAGAGTATCGTAGGC
JFB_287	ATGGAGTTTCTACGTCAACCAGAA
JFB_287_MB11B1	ATGGAGTTTTTACGTCAACCAGAG
JFB_288	TGTTATAACGATTACATGGCAGCG
JFB_365	GGAAAGAGAATGATTAAG
M13for	GTAAAACGACGGCCAG
M13rev	CAGGAAACAGCTATGAC
MB11B1_indel_for	GCTTTTTTCAGATACAAAGCCA
MB11B1_indel_rev	ATACCTGATGGAAACGACCT
MJM-154F	TAAAAAGGGAATTAATCCGC
MJM-306R	AACTCTAACCAAGAAGCA
pEVS107_3837	GGCGCGCCTAGGGCCCTC
pEVS107_3838	TCGAGGTACCTGGCCACTAG

pEVS79_for_691	GCTTGATATCGAATTCCTG
pEVS79_rev_690	TTATCGATACCGTCGACC
rev_ver_sypE	TTCACCATGAGTGCCAAATC
rscS_del1F	CTTATCTTCTAGTTCTTTTTTTTAGTGATGTCTCTTTC TACGGC
rscS_del1R	GCCGTAGAAAGAGACATCACTAAAAAAAAGAACTAG AAGATAAG
rscS_ver_1	GTAATTCAGTAATGCTACC
rscS_ver_2	GTCGCACCGTCAGGTATA
rscS_ver_3	AAGAAATTATTCGCTACC
rscS_ver_4	AGTTAGTAGGCCATTACG
SR5_syp_ver_for	TAGGCGTATCAAAAACCACCT
SR5_syp_ver_rev	TCAGGAATGTCGATGGCAG
Syp_ver_DS_rev	ATCGAGCATATTTTGCCAATC
Syp_ver_US_for	ACCTATCAACTCTTAAGTCGATTC
syp4F	TGAGGATCCCATCGTGCCATA
syp4R	AGCTCCTTTGCAATGTTTGCTT
syp5F	TATTAGGCCGTTTCCACCAGG
syp5F-B	TATTAGGTCGTTTCCATCAGG

sypA_out	AACAGGAATTGCGTTTTCAA
US_syp_flank_for	ACCACTGTGATAACTTGCAC
US_syp_flank_rev	ATGAGGCATAACCTGTTCCA

706 For Gibson assembly primers, capital letters indicate homology to the template. All primers were
707 designed for this study except MJM-154F, MJM-306R (22); JFB_287, JFB_288, and JFB_365
708 (18); and M13 for, M13 rev.
709
710 **ACKNOWLEDGMENTS**
711
712 The authors thank Elizabeth Bacon, Jacklyn Duple, Cheeneng Moua, Lynn Naughton, Olivia
713 Sauls, and Denise Tarnowski for assistance with experiments.
714
715 **FUNDING INFORMATION**
716
717 This work was funded by NIH grants R35GM119627 (to M.J.M.) and R21AI117262 (M.J.M.) and
718 NSF grant IOS-1757297 (M.J.M.). Support for trainees was provided on NIGMS grants
719 T32GM008061 (J.F.B.) and T32GM008349 (K.M.B.). This work was funded by the Chicago
720 Biomedical Consortium with support from the Searle Funds at The Chicago Community Trust
721 (supporting E.R.R.).
722
723 **REFERENCES**

724 1. Long SR. 1996. *Rhizobium* symbiosis: nod factors in perspective. Plant Cell 8:1885–1898.

725 2. Roche P, Maillet F, Plazanet C, Debellé F, Ferro M, Truchet G, Promé JC, Dénarié J. 1996.

The common *nodABC* genes of *Rhizobium meliloti* are host-range determinants. Proc Natl Acad Sci U S A 93:15305–15310.

3. Costello EK, Lauber CL, Hamady M, Fierer N, Gordon JI, Knight R. 2009. Bacterial community variation in human body habitats across space and time. Science 326:1694–1697.

4. Grice EA, Kong HH, Conlan S, Deming CB, Davis J, Young AC, NISC Comparative Sequencing Program, Bouffard GG, Blakesley RW, Murray PR, Green ED, Turner ML, Segre JA. 2009. Topographical and temporal diversity of the human skin microbiome. Science 324:1190–1192.

5. Mark Welch JL, Rossetti BJ, Rieken CW, Dewhirst FE, Borisy GG. 2016. Biogeography of a human oral microbiome at the micron scale. Proc Natl Acad Sci U S A 113:E791–E800.

6. Ruby EG. 2008. Symbiotic conversations are revealed under genetic interrogation. Nat Rev Microbiol 6:752–762.

7. Nyholm SV, McFall-Ngai MJ. 2004. The winnowing: establishing the squid-vibrio symbiosis. Nat Rev Microbiol 2:632–642.

8. Visick KL, Ruby EG. 2006. *Vibrio fischeri* and its host: it takes two to tango. Curr Opin Microbiol 9:632–638.

9. Mandel MJ, Schaefer AL, Brennan CA, Heath-Heckman EAC, Deloney-Marino CR, McFall-Ngai MJ, Ruby EG. 2012. Squid-derived chitin oligosaccharides are a chemotactic signal during colonization by *Vibrio fischeri*. Appl Environ Microbiol 78:4620–4626.

10. Jones BW, Nishiguchi MK. 2004. Counterillumination in the Hawaiian bobtail squid, *Euprymna scolopes* Berry (Mollusca: Cephalopoda). Mar Biol 144:1151–1155.

748 11. Ruby EG, McFall-Ngai MJ. 1992. A squid that glows in the night: development of an animal-
749 bacterial mutualism. J Bacteriol 174:4865–4870.

750 12. Wier AM, Nyholm SV, Mandel MJ, Massengo-Tiassé RP, Schaefer AL, Koroleva I, Splinter-
751 Bondurant S, Brown B, Manzella L, Snir E, Almabrazi H, Scheetz TE, Bonaldo M de F,
752 Casavant TL, Soares MB, Cronan JE, Reed JL, Ruby EG, McFall-Ngai MJ. 2010.
753 Transcriptional patterns in both host and bacterium underlie a daily rhythm of anatomical
754 and metabolic change in a beneficial symbiosis. Proc Natl Acad Sci U S A 107:2259–2264.

755 13. Visick KL. 2009. An intricate network of regulators controls biofilm formation and
756 colonization by *Vibrio fischeri*. Mol Microbiol 74:782–789.

757 14. Yip ES, Grublesky BT, Hussa EA, Visick KL. 2005. A novel, conserved cluster of genes
758 promotes symbiotic colonization and σ^{54}-dependent biofilm formation by *Vibrio fischeri*. Mol
759 Microbiol 57:1485–1498.

760 15. Yip ES, Geszvain K, DeLoney-Marino CR, Visick KL. 2006. The symbiosis regulator RscS
761 controls the *syp* gene locus, biofilm formation and symbiotic aggregation by *Vibrio fischeri*.
762 Mol Microbiol 62:1586–1600.

763 16. Shibata S, Yip ES, Quirke KP, Ondrey JM, Visick KL. 2012. Roles of the Structural
764 Symbiosis Polysaccharide (*syp*) Genes in Host Colonization, Biofilm Formation, and
765 Polysaccharide Biosynthesis in *Vibrio fischeri*. J Bacteriol 194:6736–6747.

766 17. Morris AR, Visick KL. 2013. The response regulator SypE controls biofilm formation and
767 colonization through phosphorylation of the syp-encoded regulator SypA in *Vibrio fischeri*.
768 Mol Microbiol 87:509–525.

769 18. Brooks JF 2nd, Mandel MJ. 2016. The Histidine Kinase BinK Is a Negative Regulator of
770 Biofilm Formation and Squid Colonization. J Bacteriol 198:2596–2607.

771 19. Tischler AH, Lie L, Thompson CM, Visick KL. 2018. Discovery of Calcium as a Biofilm-
772 Promoting Signal for Vibrio fischeri Reveals New Phenotypes and Underlying Regulatory
773 Complexity. J Bacteriol 200:e00016–18.

774 20. Pankey MS, Foxall RL, Ster IM, Perry LA, Schuster BM, Donner RA, Coyle M, Cooper VS,
775 Whistler CA. 2017. Host-selected mutations converging on a global regulator drive an
776 adaptive leap towards symbiosis in bacteria. Elife 6:e24414.

777 21. Thompson CM, Tischler AH, Tarnowski DA, Mandel MJ, Visick KL. 2018. Nitric oxide
778 inhibits biofilm formation by *Vibrio fischeri* via the nitric oxide-sensor HnoX. Mol Microbiol
779 doi:10.1111/mmi.14147.

780 22. Mandel MJ, Wollenberg MS, Stabb EV, Visick KL, Ruby EG. 2009. A single regulatory gene
781 is sufficient to alter bacterial host range. Nature 458:215–218.

782 23. Nyholm SV, Nishiguchi MK. 2008. The evolutionary ecology of a sepiolid squid-vibrio
783 association: from cell to environment. Vie Milieu Paris 58:175–184.

784 24. Fidopiastis PM, von Boletzky S, Ruby EG. 1998. A new niche for *Vibrio logei*, the
785 predominant light organ symbiont of squids in the genus *Sepiola*. J Bacteriol 180:59–64.

786 25. Ruby EG, Lee KH. 1998. The *Vibrio fischeri-Euprymna scolopes* Light Organ Association:
787 Current Ecological Paradigms. Appl Environ Microbiol 64:805–812.

788 26. Mandel MJ. 2010. Models and approaches to dissect host-symbiont specificity. Trends
789 Microbiol 18:504–511.

790 27. Gyllborg MC, Sahl JW, Cronin DC 3rd, Rasko DA, Mandel MJ. 2012. Draft genome
791 sequence of *Vibrio fischeri* SR5, a strain isolated from the light organ of the Mediterranean
792 squid *Sepiola robusta*. J Bacteriol 194:1639.

793 28. Geszvain K, Visick KL. 2008. Multiple factors contribute to keeping levels of the symbiosis
794 regulator RscS low. FEMS Microbiol Lett 285:33–39.

795 29. Wollenberg MS, Ruby EG. 2009. Population structure of *Vibrio fischeri* within the light
796 organs of *Euprymna scolopes* squid from Two Oahu (Hawaii) populations. Appl Environ
797 Microbiol 75:193–202.

798 30. Wollenberg MS, Ruby EG. 2012. Phylogeny and fitness of *Vibrio fischeri* from the light
799 organs of *Euprymna scolopes* in two Oahu, Hawaii populations. ISME J 6:352–362.

800 31. Elliott KT, DiRita VJ. 2008. Characterization of CetA and CetB, a bipartite energy taxis
801 system in *Campylobacter jejuni*. Mol Microbiol 69:1091–1103.

802 32. Antonov I, Coakley A, Atkins JF, Baranov PV, Borodovsky M. 2013. Identification of the
803 nature of reading frame transitions observed in prokaryotic genomes. Nucleic Acids Res
804 41:6514–6530.

805 33. Bongrand C, Koch EJ, Moriano-Gutierrez S, Cordero OX, McFall-Ngai M, Polz MF, Ruby
806 EG. 2016. A genomic comparison of 13 symbiotic *Vibrio fischeri* isolates from the
807 perspective of their host source and colonization behavior. ISME J 10:2907–2917.

808 34. Altschul SF, Madden TL, Schäffer AA, Zhang J, Zhang Z, Miller W, Lipman DJ. 1997.
809 Gapped BLAST and PSI-BLAST: a new generation of protein database search programs.
810 Nucleic Acids Res 25:3389–3402.

811 35. Rusch DB, Rowe-Magnus DA. 2017. Complete Genome Sequence of the Pathogenic
812 *Vibrio vulnificus* Type Strain ATCC 27562. Genome Announc 5:e00907–17.

813 36. Morris AR, Darnell CL, Visick KL. 2011. Inactivation of a novel response regulator is
814 necessary for biofilm formation and host colonization by *Vibrio fischeri*. Mol Microbiol

815 82:114–130.

816 37. Guo Y, Rowe-Magnus DA. 2011. Overlapping and unique contributions of two conserved
817 polysaccharide loci in governing distinct survival phenotypes in Vibrio vulnificus. Environ
818 Microbiol 13:2888–2990.

819 38. Morris AR, Visick KL. 2013. Inhibition of SypG-induced biofilms and host colonization by the
820 negative regulator SypE in *Vibrio fischeri*. PLoS One 8:e60076.

821 39. Hussa EA, Darnell CL, Visick KL. 2008. RscS functions upstream of SypG to control the
822 syp locus and biofilm formation in *Vibrio fischeri*. J Bacteriol 190:4576–4583.

823 40. Koehler S, Gaedeke R, Thompson C, Bongrand C, Visick KL, Ruby E, McFall-Ngai M.
824 2018. The model squid-vibrio symbiosis provides a window into the impact of strain- and
825 species-level differences during the initial stages of symbiont engagement. Environ
826 Microbiol doi:10.1111/1462–2920.14392.

827 41. Ray VA, Visick KL. 2012. LuxU connects quorum sensing to biofilm formation in *Vibrio*
828 *fischeri*. Mol Microbiol 86:954–970.

829 42. Giraud E, Moulin L, Vallenet D, Barbe V, Cytryn E, Avarre J-C, Jaubert M, Simon D,
830 Cartieaux F, Prin Y, Bena G, Hannibal L, Fardoux J, Kojadinovic M, Vuillet L, Lajus A,
831 Cruveiller S, Rouy Z, Mangenot S, Segurens B, Dossat C, Franck WL, Chang W-S,
832 Saunders E, Bruce D, Richardson P, Normand P, Dreyfus B, Pignol D, Stacey G, Emerich
833 D, Verméglio A, Médigue C, Sadowsky M. 2007. Legumes symbioses: absence of Nod
834 genes in photosynthetic bradyrhizobia. Science 316:1307–1312.

835 43. Bonaldi K, Gargani D, Prin Y, Fardoux J, Gully D, Nouwen N, Goormachtig S, Giraud E.
836 2011. Nodulation of *Aeschynomene afraspera* and *A. indica* by photosynthetic
837 *Bradyrhizobium* Sp. strain ORS285: the Nod-dependent versus the Nod-independent

symbiotic interaction. Mol Plant Microbe Interact 24:1359–1371.

44. Darriba D, Taboada GL, Doallo R, Posada D. 2012. jModelTest 2: more models, new heuristics and parallel computing. Nat Methods 9:772.

45. Swofford DL. 2003. PAUP*: Phylogenetic Analysis Using Parsimony (* and Other Methods) 4th edn. Sinauer.

46. Ronquist F, Teslenko M, van der Mark P, Ayres DL, Darling A, Höhna S, Larget B, Liu L, Suchard MA, Huelsenbeck JP. 2012. MrBayes 3.2: efficient Bayesian phylogenetic inference and model choice across a large model space. Syst Biol 61:539–542.

47. Ronquist F, van der Mark P, Huelsenbeck JP. 2009. Bayesian phylogenetic analysis using MrBayes, 2nd edn. Cambridge University Press.

48. Visick KL, Hodge-Hanson KM, Tischler AH, Bennett AK, Mastrodomenico V. 2018. Tools for Rapid Genetic Engineering of *Vibrio fischeri*. Appl Environ Microbiol 84:e00850–18.

49. Pollack-Berti A, Wollenberg MS, Ruby EG. 2010. Natural transformation of *Vibrio fischeri* requires *tfoX* and *tfoY*. Environ Microbiol 12:2302–2311.

50. Baba T, Ara T, Hasegawa M, Takai Y, Okumura Y, Baba M, Datsenko KA, Tomita M, Wanner BL, Mori H. 2006. Construction of *Escherichia coli* K-12 in-frame, single-gene knockout mutants: the Keio collection. Mol Syst Biol 2:2006.0008.

51. Naughton LM, Mandel MJ. 2012. Colonization of *Euprymna scolopes* squid by *Vibrio fischeri*. J Vis Exp e3758.

52. Finn RD, Coggill P, Eberhardt RY, Eddy SR, Mistry J, Mitchell AL, Potter SC, Punta M, Qureshi M, Sangrador-Vegas A, Salazar GA, Tate J, Bateman A. 2016. The Pfam protein families database: towards a more sustainable future. Nucleic Acids Res 44:D279–85.

860 53. Lee K-H. 1994. Ecology of *Vibrio fisheri*: the light organ symbiont of the Hawaiian sepiolid
861 squid *Euprymna scolopes*. University of Southern California.

862 54. Boettcher KJ, Ruby EG. 1990. Depressed light emission by symbiotic *Vibrio fischeri* of the
863 sepiolid squid *Euprymna scolopes*. J Bacteriol 172:3701–3706.

864 55. Boettcher KJ, Ruby EG. 1994. Occurrence of plasmid DNA in the sepiolid squid symbiont
865 *Vibrio fischeri*. Curr Microbiol 29:279–286.

866 56. Nishiguchi MK, Ruby EG, McFall-Ngai MJ. 1998. Competitive dominance among strains of
867 luminous bacteria provides an unusual form of evidence for parallel evolution in Sepiolid
868 squid-vibrio symbioses. Appl Environ Microbiol 64:3209–3213.

869 57. Nishiguchi MK, Nair VS. 2003. Evolution of symbiosis in the Vibrionaceae: a combined
870 approach using molecules and physiology. Int J Syst Evol Microbiol 53:2019–2026.

871 58. Stabb EV, Ruby EG. 2002. RP4-based plasmids for conjugation between *Escherichia coli*
872 and members of the *Vibrionaceae*. Methods Enzymol 358:413–426.

873 59. Dunn AK, Millikan DS, Adin DM, Bose JL, Stabb EV. 2006. New *rfp*- and pES213-derived
874 tools for analyzing symbiotic *Vibrio fischeri* reveal patterns of infection and *lux* expression in
875 situ. Appl Environ Microbiol 72:802–810.

876 60. Visick KL, Skoufos LM. 2001. Two-component sensor required for normal symbiotic
877 colonization of *Euprymna scolopes* by *Vibrio fischeri*. J Bacteriol 183:835–842.

878 61. McCann J, Stabb EV, Millikan DS, Ruby EG. 2003. Population dynamics of *Vibrio fischeri*
879 during infection of *Euprymna scolopes*. Appl Environ Microbiol 69:5928–5934.

880

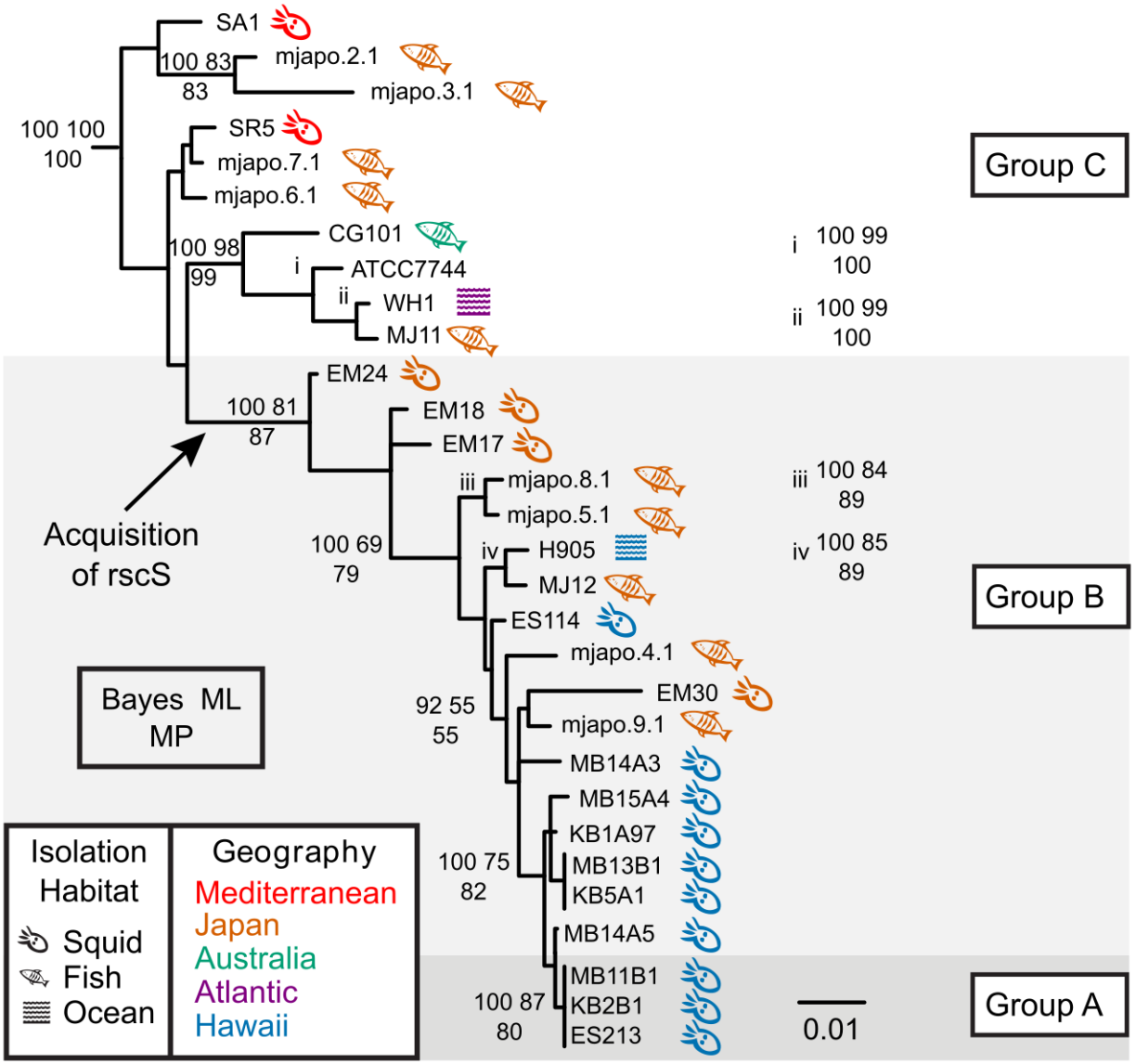
SA1
mjapo.2.1
mjapo.3.1
100 83
83
100 100
100
SR5
mjapo.7.1
mjapo.6.1
CG101
ATCC7744
WH1
MJ11
100 98
99
i
ii
EM24
EM18
EM17
100 81
87
mjapo.8.1
mjapo.5.1
H905
MJ12
ES114
100 69
79
iii
iv
mjapo.4.1
EM30
mjapo.9.1
MB14A3
MB15A4
KB1A97
MB13B1
KB5A1
MB14A5
MB11B1
KB2B1
ES213
92 55
55
100 75
82
100 87
80
i 100 99
100
ii 100 99
100
iii 100 84
89
iv 100 85
89
Group C
Group B
Group A
Acquisition
of rscS
Bayes ML
MP
Isolation
Habitat
Squid
Fish
Ocean
Geography
Mediterranean
Japan
Australia
Atlantic
Hawaii
0.01

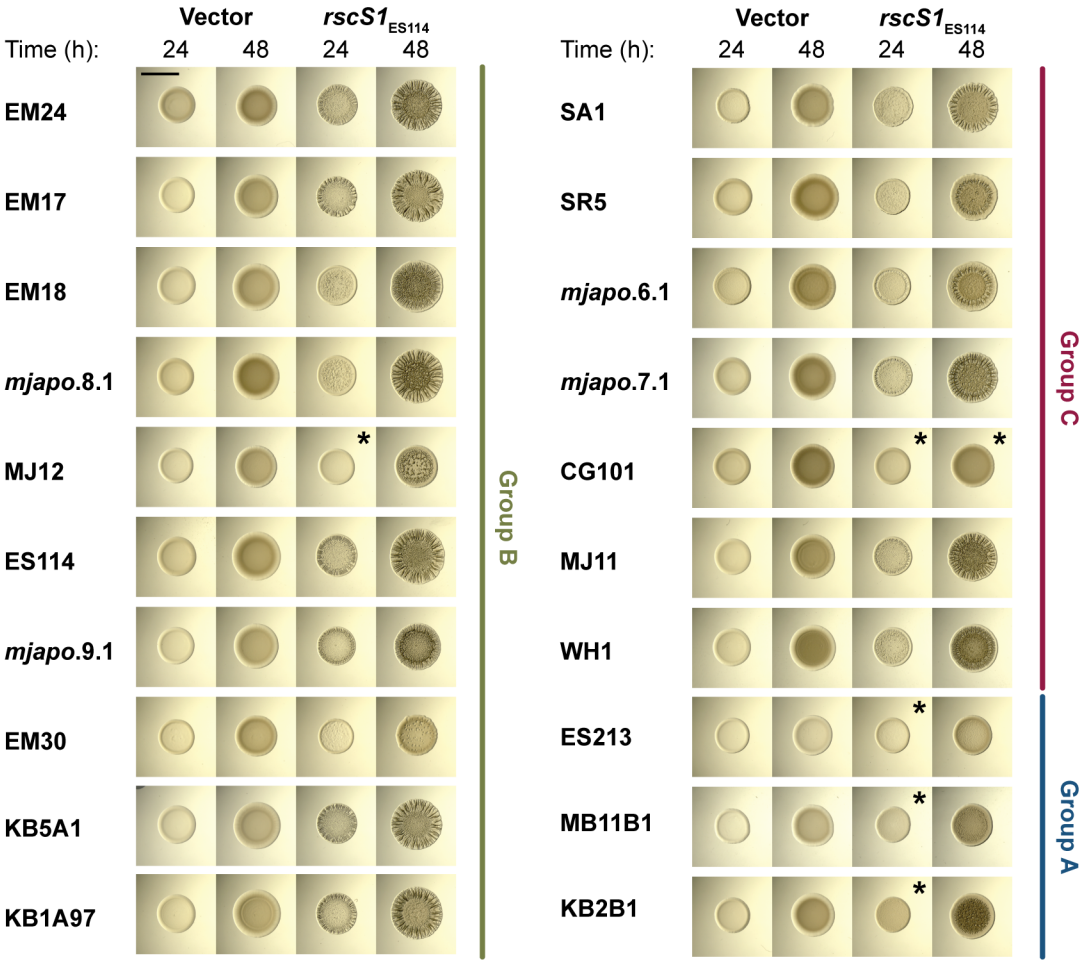
Vector
rscS1ES114
Time (h):
24
48
24
48
EM24
EM17
EM18
mjapo.8.1
MJ12
ES114
mjapo.9.1
EM30
KB5A1
KB1A97
Group B
SA1
SR5
mjapo.6.1
mjapo.7.1
CG101
MJ11
WH1
ES213
MB11B1
KB2B1
Group C
Group A

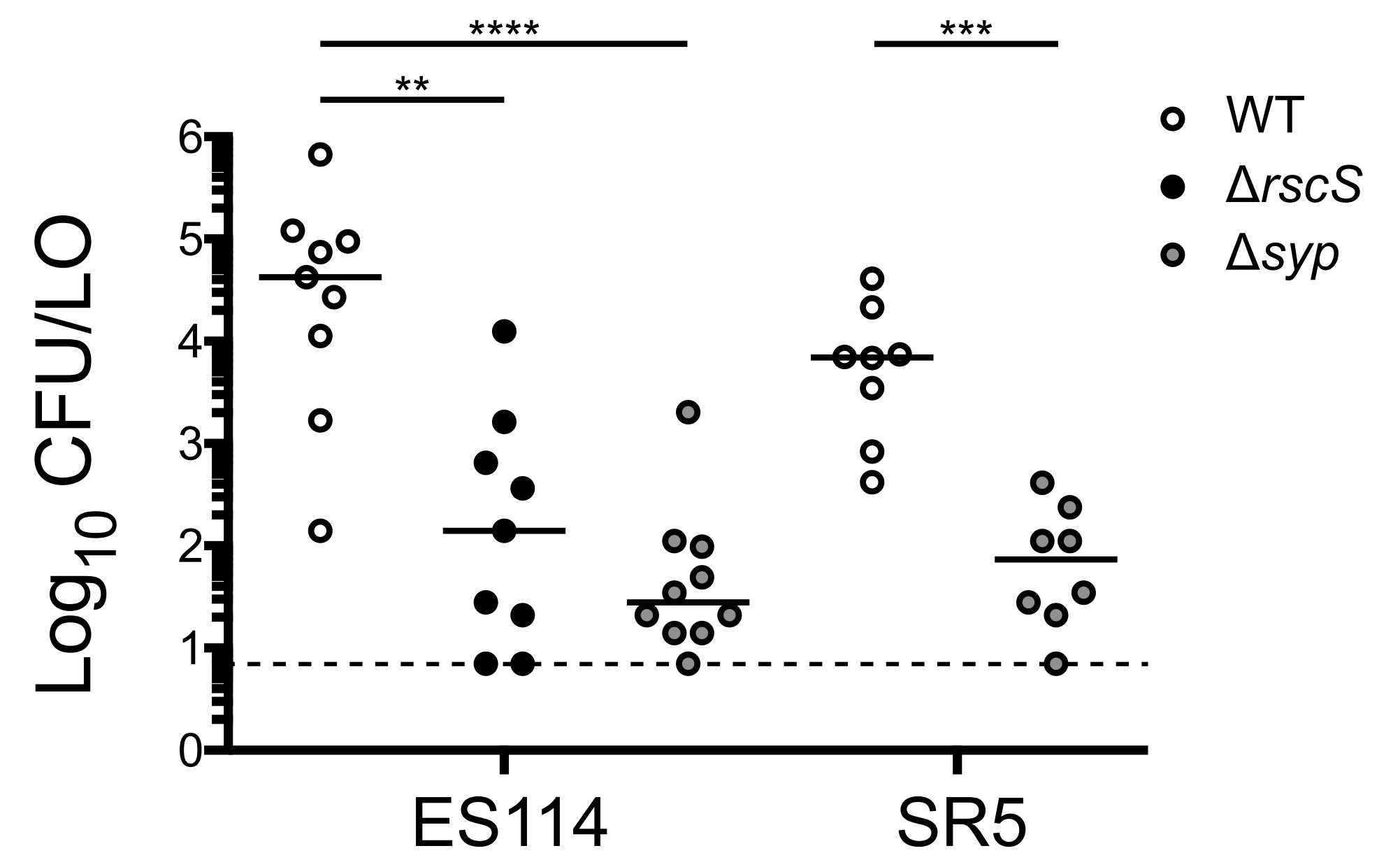
****
***
**
WT
ΔrscS
Δsyp
Log10 CFU/LO
6
5
4
3
2
1
0
ES114
SR5

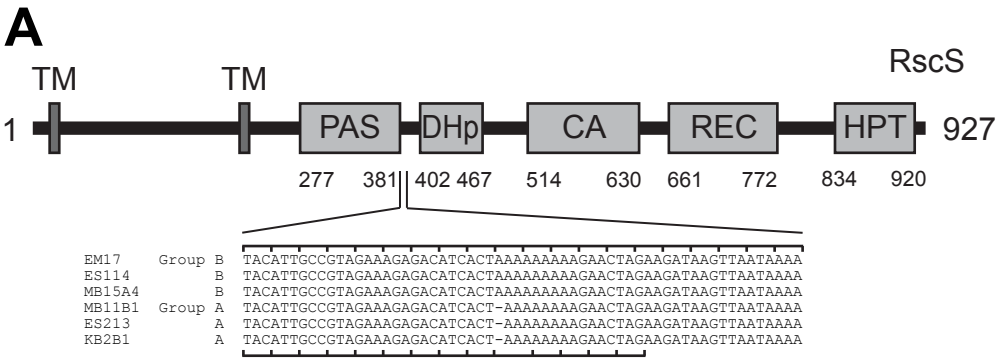
A
TM
TM
RscS
1
PAS
DHp
CA
REC
HPT
927
277
381
402
467
514
630
661
772
834
920
EM17 Group B TACATTGCCGTAGAAAGAGACATCACTAAAAAAAAAAGAACTAGAAGATAAGTTAATAAAA
ES114 B TACATTGCCGTAGAAAGAGACATCACTAAAAAAAAAAGAACTAGAAGATAAGTTAATAAAA
MB15A4 B TACATTGCCGTAGAAAGAGACATCACTAAAAAAAAAAGAACTAGAAGATAAGTTAATAAAA
MB11B1 Group A TACATTGCCGTAGAAAGAGACATCACT-AAAAAAAAAGAACTAGAAGATAAGTTAATAAAA
ES213 A TACATTGCCGTAGAAAGAGACATCACT-AAAAAAAAAGAACTAGAAGATAAGTTAATAAAA
KB2B1 A TACATTGCCGTAGAAAGAGACATCACT-AAAAAAAAAGAACTAGAAGATAAGTTAATAAAA

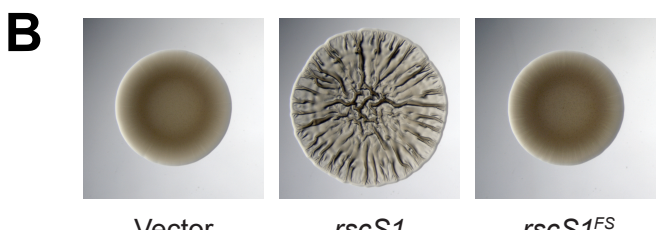
B
Vector
rscS1
rscS1FS

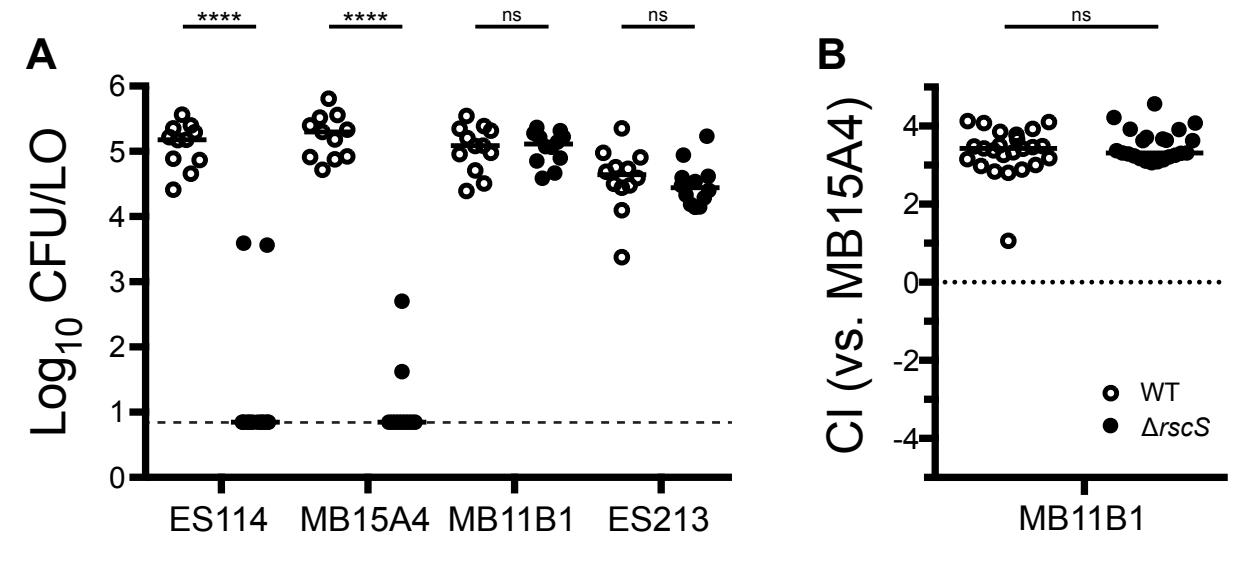
A
B
****
****
ns
ns
ns
Log10 CFU/LO
6
5
4
3
2
1
0
ES114
MB15A4
MB11B1
ES213
CI (vs. MB15A4)
4
2
0
-2
-4
WT
ΔrscS
MB11B1

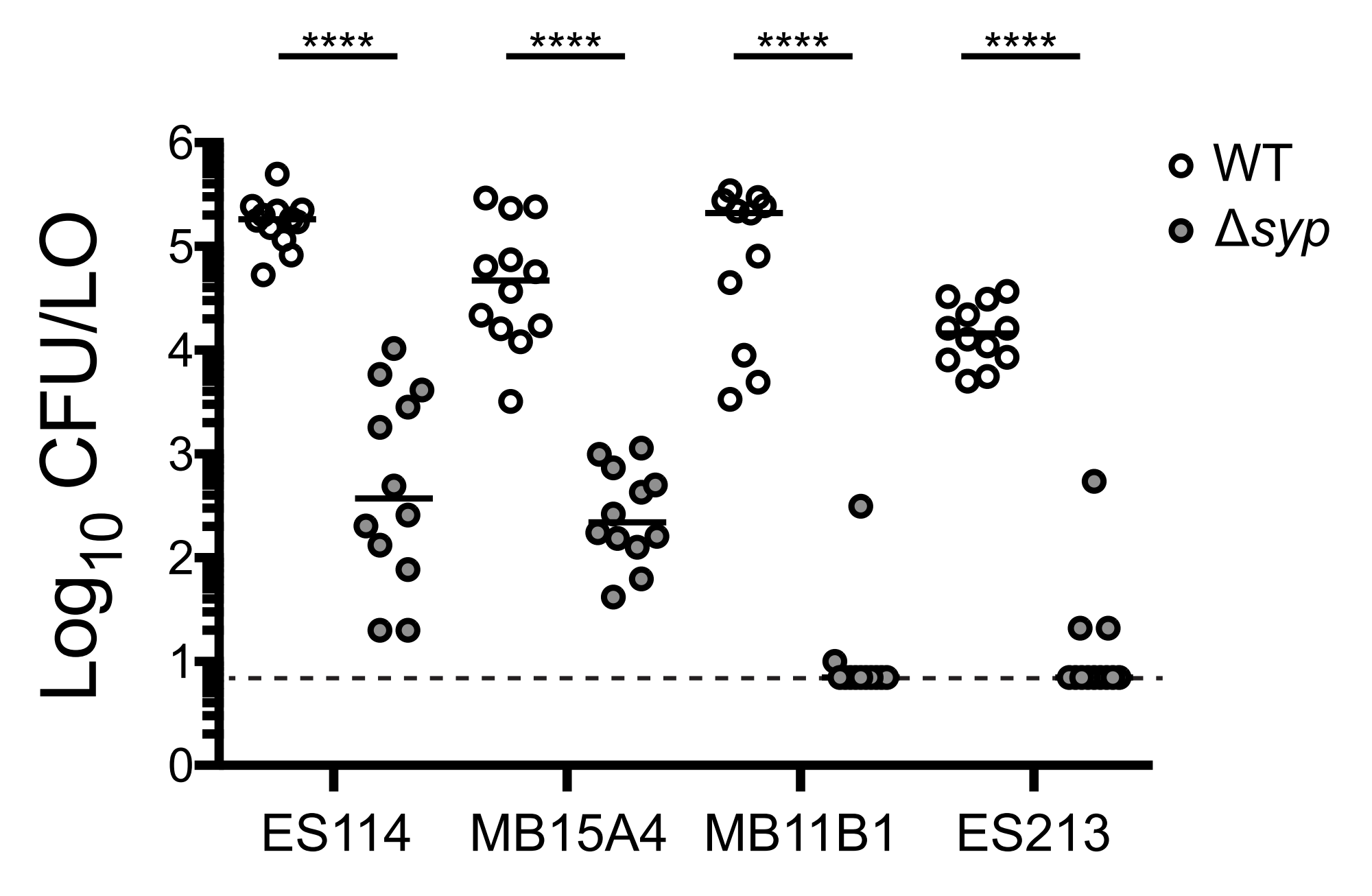
****
****
****
****
Log10 CFU/LO
6
5
4
3
2
1
0
WT
Δsyp
ES114
MB15A4
MB11B1
ES213

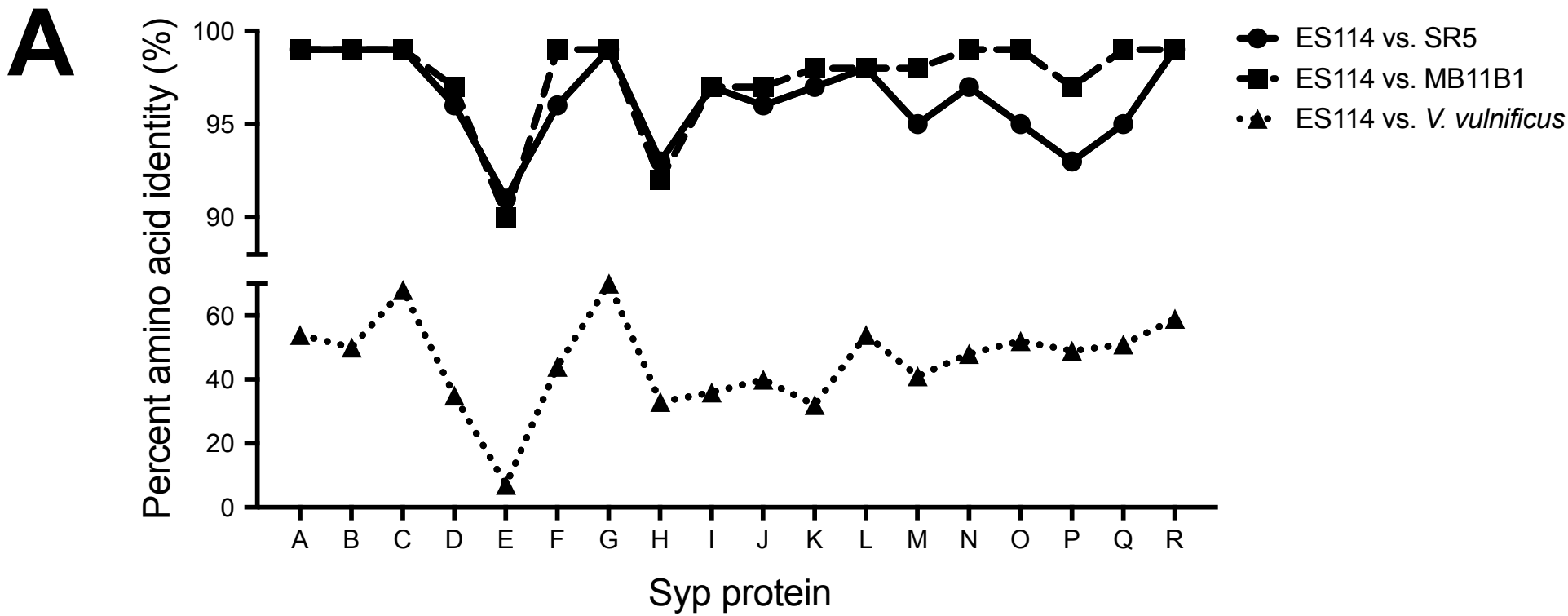
A
Percent amino acid identity (%)
100
95
90
60
40
20
0
A B C D E F G H I J K L M N O P Q R
Syp protein
ES114 vs. SR5
ES114 vs. MB11B1
ES114 vs. V. vulnificus

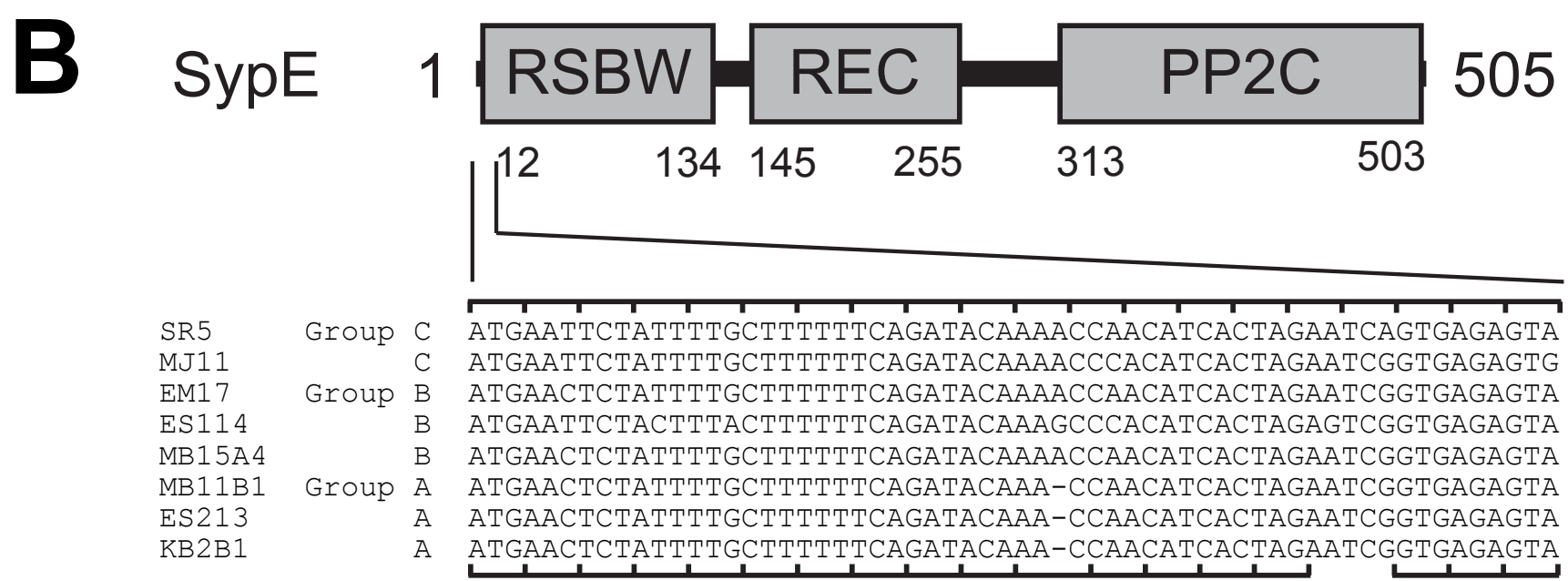
B
SypE
1
RSBW
REC
PP2C
505
12
134
145
255
313
503
SR5 Group C ATGAATTCTATTTTGCTTTTTTCAGATACAAAACCAACATCACTAGAATCAGTGAGAGTA
MJ11 C ATGAATTCTATTTTGCTTTTTTCAGATACAAAACCCACATCACTAGAATCGGTGAGAGTG
EM17 Group B ATGAACTCTATTTTGCTTTTTTCAGATACAAAACCAACATCACTAGAATCGGTGAGAGTA
ES114 B ATGAATTCTACTTTACTTTTTTCAGATACAAAGCCCACATCACTAGAGTCGGTGAGAGTA
MB15A4 B ATGAACTCTATTTTGCTTTTTTCAGATACAAAACCAACATCACTAGAATCGGTGAGAGTA
MB11B1 Group A ATGAACTCTATTTTGCTTTTTTCAGATACAAA-CCAACATCACTAGAATCGGTGAGAGTA
ES213 A ATGAACTCTATTTTGCTTTTTTCAGATACAAA-CCAACATCACTAGAATCGGTGAGAGTA
KB2B1 A ATGAACTCTATTTTGCTTTTTTCAGATACAAA-CCAACATCACTAGAATCGGTGAGAGTA

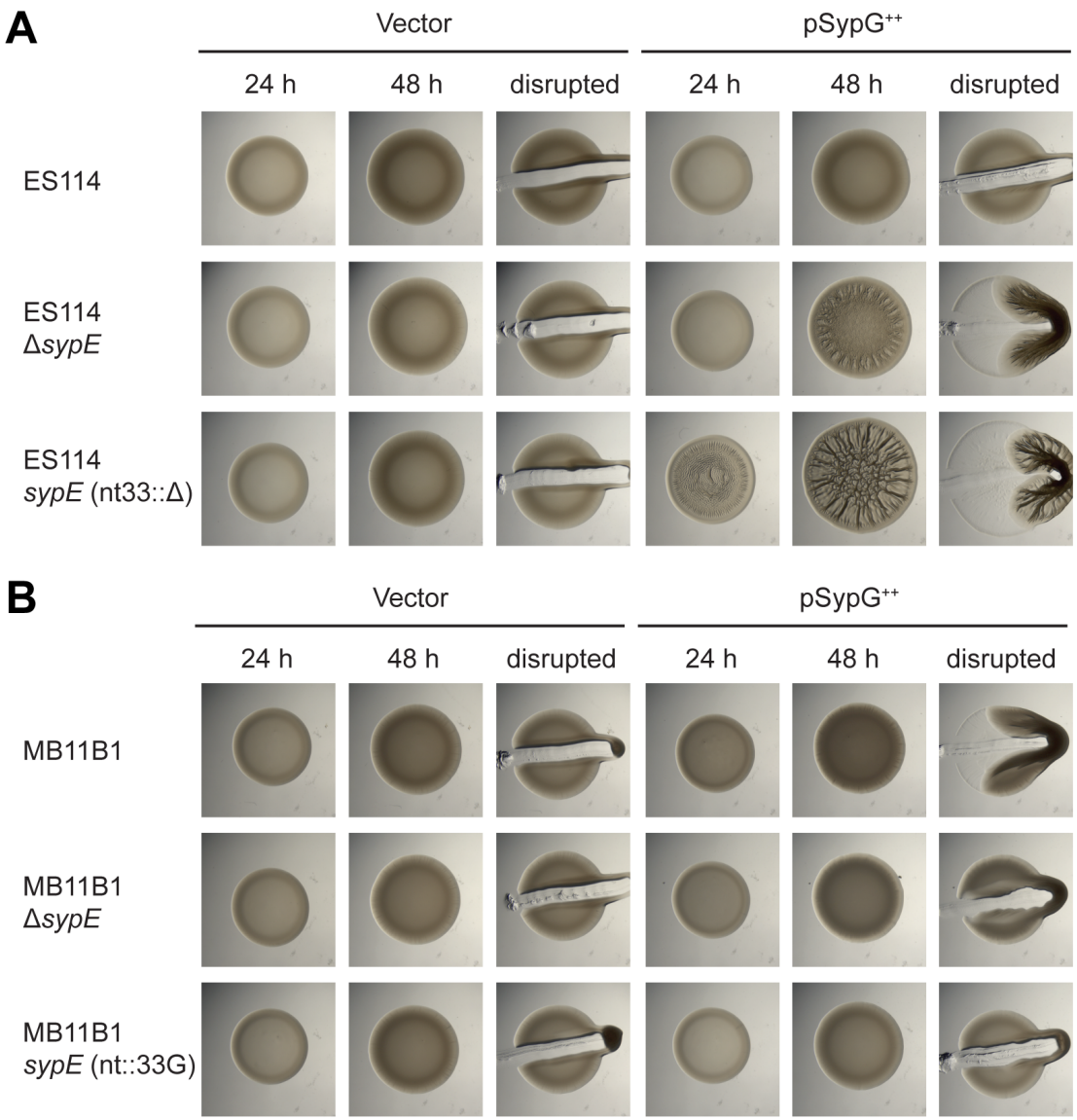
A
Vector
pSypG++
24 h
48 h
disrupted
24 h
48 h
disrupted
ES114
ES114
ΔsypE
ES114
sypE (nt33::Δ)
B
Vector
pSypG++
24 h
48 h
disrupted
24 h
48 h
disrupted
MB11B1
MB11B1
ΔsypE
MB11B1
sypE (nt::33G)

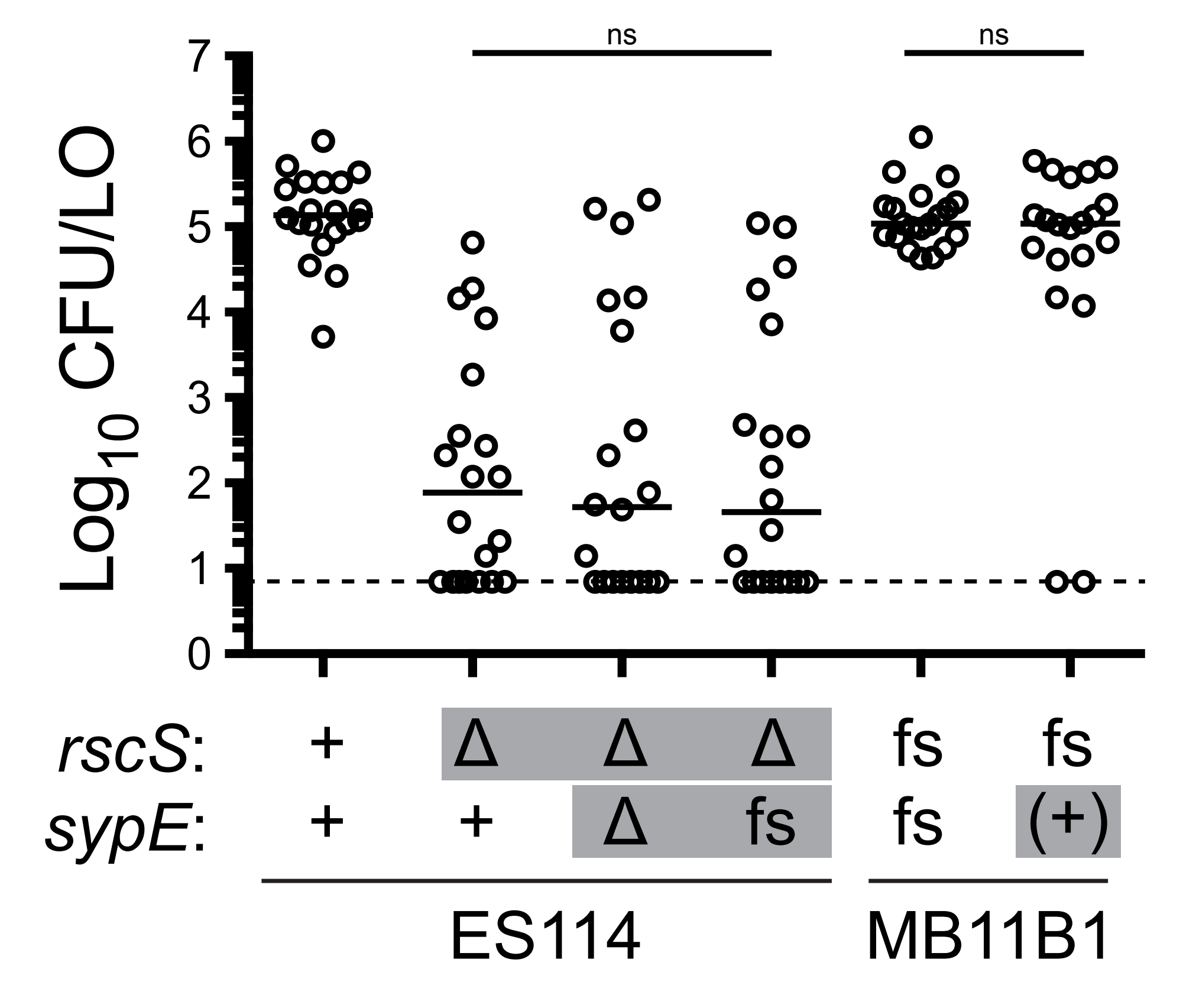
ns
ns
7
6
5
4
3
2
1
0
Log10 CFU/LO
rscS:
+
Δ
Δ
Δ
fs
fs
sypE:
+
+
Δ
fs
fs
(+)
ES114
MB11B1

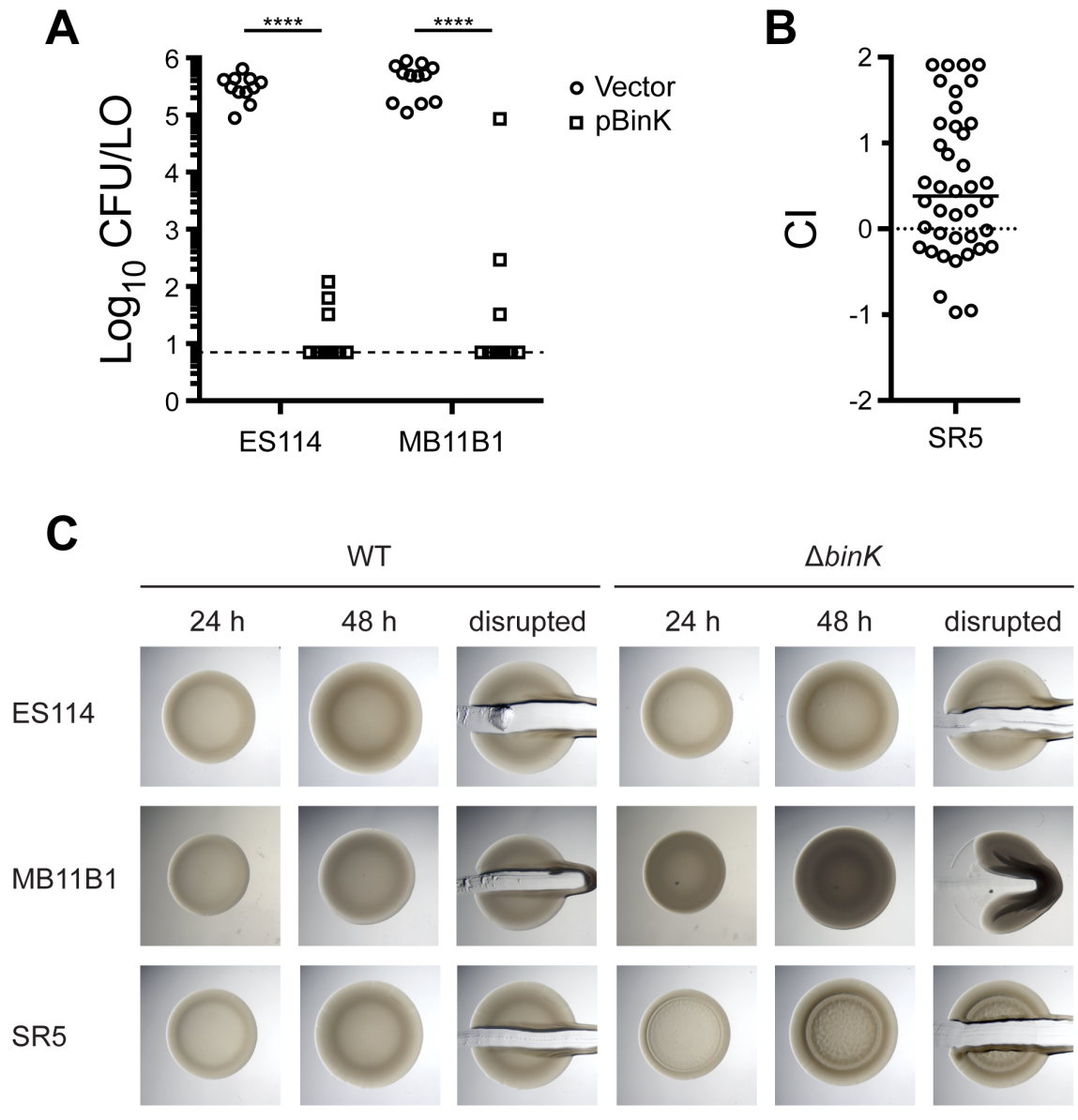
A
****
****
Log10 CFU/LO
6
5
4
3
2
1
0
Vector
pBinK
ES114
MB11B1
B
CI
2
1
0
-1
-2
SR5
C
WT
ΔbinK
24 h
48 h
disrupted
24 h
48 h
disrupted
ES114
MB11B1
SR5

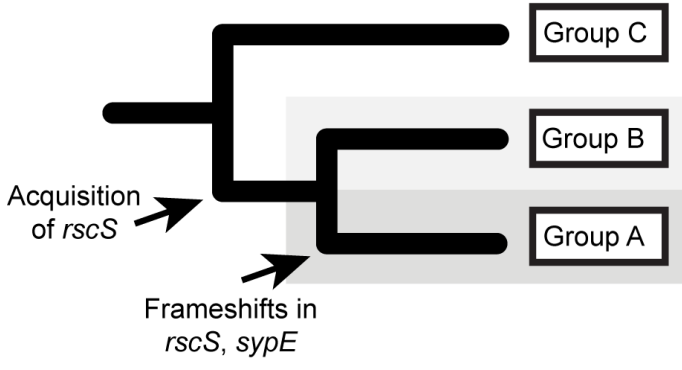

	rscS	**Colonization: RscS**	***sypE***	**Biofilm: BinK**
Group C	No	Not required	Yes	Negative regulator
Group B	Yes	Required	Yes	Negative regulator
Group A	ntA1141Δ	Not required	ntG33Δ	Negative regulator

Table S1. Primers pairs for construction of mutants.

Strain	Note	Forward Primer	Reverse Primer	PCR Product Size	Description of PCR product	E. coli with clone
MJM3010 =		Gib_ES114_rscS_US_for	Gib_ES114_rscS_US_rev	1.6 kb	Gibson assembly cloning of upstream *rscS* region in MJM1100 into pEVS79	**MJM3008**
MJM1100 Δ*rscS* and		Gib_ES114_rscS_DS_for	Gib_ES114_rscS_DS_rev	1.6 kb	Gibson assembly cloning of downstream *rscS* region in MJM1100 into pEVS79	
MJM3394 =		ES114_US_ver	ES114_DS_ver	586 bp	Verification of Δ*rscS* by flanking the upstream/downstream junction	
MJM3354 Δ*rscS*		ES114_US_ver	DAT015F	520 bp	Verification of Δ*rscS*; no product due to one primer binding within *rscS*.	
		Gib_ES114_rscS_US_for	Gib_ES213_rscS_US_rev	1.6 kb	Gibson assembly cloning of upstream *rscS* region in MJM1117 into pEVS79	**MJM3014**
MJM3017 =		Gib_ES114_rscS_DS_for	Gib_ES114_rscS_DS_rev	1.6 kb	Gibson assembly cloning of downstream *rscS* region in MJM1117 into pEVS79	
MJM1117 Δ*rscS*		ES114_US_ver	ES114_DS_ver	586 bp	Verification of Δ*rscS* by flanking the upstream/downstream junction	
		ES114_US_ver	DAT015F	520 bp	Verification of Δ*rscS*; no product due to one primer binding within *rscS*.	
		Gib_ES114_rscS_US_for	Gib_ES114_rscS_US_rev	1.6 kb	Gibson assembly cloning of upstream *rscS* region in MJM1130 into pEVS79	**MJM3043**
MJM3046 =		Gib_ES114_rscS_DS_for	Gib_ES114_rscS_DS_rev	1.6 kb	Gibson assembly cloning of downstream *rscS* region in MJM1130 into pEVS79	
MJM1130 Δ*rscS*		ES114_US_ver	ES114_DS_ver	586 bp	Verification of Δ*rscS* by flanking the upstream/downstream junction	
		ES114_US_ver	DAT015F	520 bp	Verification of Δ*rscS*; no product due to one primer binding within *rscS*	
		Gib_ES114_rscS_US_for	Gib_ES114_rscS_US_rev	1.6 kb	Gibson assembly cloning of upstream *rscS* region in MJM2114 into pEVS79	**MJM3039**
MJM3042 =		Gib_ES114_rscS_DS_for	Gib_ES114_rscS_DS_rev	1.6 kb	Gibson assembly cloning of downstream *rscS* region in MJM2114 into pEVS79	
MJM2114 Δ*rscS*		ES114_US_ver	ES114_DS_ver	586 bp	Verification of Δ*rscS* by flanking the upstream/downstream junction	
		ES114_US_ver	DAT015F	520 bp	Verification of Δ*rscS*; no product due to one primer binding within *rscS*	
		Gib_ES114_syp_US_for	Gib_ES114_syp_US_rev	1.6 kb	Gibson assembly cloning of upstream *sypA* region in MJM1100 into pEVS79	**MJM3060**
MJM3062 =		Gib_ES114_syp_DS_for	Gib_ES114_syp_DS_rev	1.6 kb	Gibson assembly cloning of downstream *sypR* region in MJM1100 into pEVS79	
MJM1100 Δ*sypA-R*		Syp_ver_US_for	Syp_ver_DS_rev	503 bp	Verification of Δ*sypA-R* by flanking the upstream/downstream junction	
		Syp_ver_US_for	sypA_out	490 bp	Verification of Δ*sypA-R*; no product due to one primer binding within *sypA*	
		Gib_ES114_syp_US_for	Gib_ES114_syp_US_rev	1.6 kb	Gibson assembly cloning of upstream *sypA* region in MJM1117 into pEVS79	**MJM3066**
MJM3068 =		Gib_MB11B1_syp_DS_for	Gib_ES114_syp_DS_rev	1.6 kb	Gibson assembly cloning of downstream *sypR* region in MJM1117 into pEVS79	
MJM1117 Δ*sypA-R*		Syp_ver_US_for	Syp_ver_DS_rev	503 bp	Verification of Δ*sypA-R* by flanking the upstream/downstream junction	
		Syp_ver_US_for	sypA_out	490 bp	Verification of Δ*sypA-R*; no product due to one primer binding within *sypA*	
		Gib_SR5_syp_US_for	Gib_SR5_syp_US_rev	1.6 kb	Gibson assembly cloning of upstream *sypA* region in MJM1125 into pEVS79	**MJM3500**
MJM3501 =		Gib_SR5_syp_DS_for	Gib_SR5_syp_DS_rev	1.6 kb	Gibson assembly cloning of downstream *sypR* region in MJM1125 into pEVS79	
MJM1125 Δ*sypA-R*		SR5_syp_ver_for	SR5_syp_ver_rev	506 bp	Verification of Δ*sypA-R* by flanking the upstream/downstream junction	
		Gib_SR5_syp_US_for	sypA_out	1.9 kb	Verification of Δ*sypA-R*; no product due to one primer binding within *sypA*	
		Gib_MB11B1_syp_US_for	Gib_MB11B1_syp_US_rev	1.6 kb	Gibson assembly cloning of upstream *sypA* region in MJM1130 into pEVS79	**MJM3063**
MJM3065 =		Gib_MB11B1_syp_DS_for	Gib_ES114_syp_DS_rev	1.6 kb	Gibson assembly cloning of downstream *sypR* region in MJM1130 into pEVS79	
MJM1130 Δ*sypA-R*		Syp_ver_US_for	Syp_ver_DS_rev	503 bp	Verification of Δ*sypA-R* by flanking the upstream/downstream junction	
		Syp_ver_US_for	sypA_out	490 bp	Verification of Δ*sypA-R*; no product due to one primer binding within *sypA*	
		Gib_ES114_syp_US_for	Gib_ES114_syp_US_rev	1.6 kb	Gibson assembly cloning of upstream *sypA* region in MJM2114 into pEVS79	**MJM3069**
MJM3071 =		Gib_ES114_syp_DS_for	Gib_ES114_syp_DS_rev	1.6 kb	Gibson assembly cloning of downstream *sypR* region in MJM2114 into pEVS79	
MJM2114 Δ*sypA-R*		Syp_ver_US_for	Syp_ver_DS_rev	503 bp	Verification of Δ*sypA-R* by flanking the upstream/downstream junction	
		Syp_ver_US_for	sypA_out	490 bp	Verification of Δ*sypA-R*; no product due to one primer binding within *sypA*	
		Gib_ES114_binK_US_for	Gib_ES114_binK_US_rev	1.6 kb	Gibson assembly cloning of upstream *binK* region in MJM1130 into pEVS79	**MJM3082**
MJM3084 =		Gib_ES114_binK_DS_for	Gib_ES114_binK_DS_rev	1.6 kb	Gibson assembly cloning of downstream *binK* region in MJM1130 into pEVS79	
MJM1130 Δ*binK*		JFB_287_MB11B1	JFB_288	767 bp	Verification of Δ*binK* by flanking the upstream/downstream junction	
		JFB_287_MB11B1	JFB_365	624 bp	Verification of Δ*binK*; no product due to one primer binding within *binK*	
MJM3417 =		Gib_ES114_sypE_US_for	Gib_ES114_sypE_US_rev	1.6 kb	Gibson assembly cloning of upstream *sypE* region in MJM1100 into pEVS79	**MJM3416**
MJM1100 Δ*sypE* and		Gib_ES114_sypE_DS_for	Gib_ES114_sypE_DS_rev	1.6 kb	Gibson assembly cloning of downstream *sypE* region in MJM1100 into pEVS79	
MJM3423 =		syp4F	syp4R	780 bp	Verification of Δ*sypE* by flanking the upstream/downstream junction	
MJM3010 Δ*sypE*		syp5F	syp4R	772 bp	Verification of Δ*sypE*; no product due to one primer binding within *sypE*	
		Gib_MB11B1_sypE_US_for	Gib_MB11B1_sypE_US_rev	1.6 kb	Gibson assembly cloning of upstream *sypE* region in MJM1130 into pEVS79	**MJM3409**
MJM3410 =		Gib_MB11B1_sypE_DS_for	Gib_MB11B1_sypE_DS_rev	1.6 kb	Gibson assembly cloning of downstream *sypE* region in MJM1130 into pEVS79	
MJM1130 Δ*sypE*		for_ver_sypE	rev_ver_sypE	732 bp	Verification of Δ*sypE* by flanking the upstream/downstream junction	
		MB11B1_indel_for	MB11B1_indel_rev	779 bp	Verification of Δ*sypE*; no product due to both primers binding within *sypE*	
		Gib_ES114_sypE_N_for	Gib_ES114_sypE_N_rev	332 bp	Gibson assembly cloning of N-terminal *sypE* in MJM1100 into pEVS107	**MJM3340**
MJM3354 =		Gib_ES114_sypE_C_for	Gib_ES114_sypE_C_rev	1786 bp	Gibson assembly cloning of C-terminal *sypE* in MJM1100 into pEVS107	**and**
MJM1100 *sypE*(ntG33Δ)		Gib_pEVS79_ES_sypE_for	Gib_pEVS79_ES_sypE_rev	2118 bp	Gibson assembly cloning of *sypE*(ntG33Δ) into pEVS79	**MJM3352**
		ES114_indel_for	ES114_indel_rev	802 bp	Verification of *sypE*(ntG33Δ); stronger band with original allele.	
		Gib_MB11B1_sypE_N_for	Gib_MB11B1_sypE_N_rev	332 bp	Gibson assembly cloning of N-terminal *sypE* in MJM1130 into pEVS107	**MJM3338**
MJM3397 =		Gib_MB11B1_sypE_C_for	Gib_MB11B1_sypE_C_rev	1786 bp	Gibson assembly cloning of C-terminal *sypE* in MJM1130 into pEVS107	**and**
MJM1130 *sypE*(nt33::G)		Gib_pEVS79_MB_sypE_for	Gib_pEVS79_MB_sypE_rev	2118 bp	Gibson assembly cloning *sypE*(nt33::G) into pEVS79	**MJM3351**
		MB11B1_indel_for	MB11B1_indel_rev	779 bp	Verification of *sypE*(nt33::G); stronger band with corrected allele.	

>gBlock_erm
GGTCAGCCTCTAATGGCTCGTAAGATAGTGTAGGAAGCTTTATCGAACTGCGCGAAAGATCCCGAAGTTCCTATTCTCT
AGAAAGTATAGGAACTTCCTTAGAAGCAAACTTAAGAGTGTGTTGATAGTGCAGTATCTTAAAATTTTGTATAATAGGA
ATTGAAGTTAAATTAGATGCTAAAAATTTGTAATTAAGAAGGAGTGATTACATGAACAAAAATATAAAATATTCTCAAA
ACTTTTTAACGAGTGAAAAAGTACTCAACCAAATAATAAAACAATTGAATTTAAAAGAAACCGATACCGTTTACGAAAT
TGGAACAGGTAAAGGGCATTTAACGACGAAACTGGCTAAAATAAGTAAACAGGTAACGTCTATTGAATTAGACAGTCAT
CTATTCAACTTATCGTCAGAAAAATTAAAACTGAATACTCGTGTCACTTTAATTCACCAAGATATTCTACAGTTTCAAT
TCCCTAACAAACAGAGGTATAAAATTGTTGGGAGTATTCCTTACCATTTAAGCACACAAATTATTAAAAAAGTGGTTTT
TGAAAGCCATGCGTCTGACATCTATCTGATTGTTGAAGAAGGATTCTACAAGCGTACCTTGGATATTCACCGAACACTA
GGGTTGCTCTTGCACACTCAAGTCTCGATTCAGCAATTGCTTAAGCTGCCAGCGGAATGCTTTCATCCTAAACCAAAAG
TAAACAGTGTCTTAATAAAACTTACCCGCCATACCACAGATGTTCCAGATAAATATTGGAAGCTATATACGTACTTTGT
TTCAAAATGGGTCAATCGAGAATATCGTCAACTGTTTACTAAAAATCAGTTTCATCAAGCAATGAAACACGCCAAAGTA
AACAATTTAAGTACCGTTACTTATGAGCAAGTATTGTCTATTTTTAATAGTTATCTATTATTTAACGGGAGGAAATAAT
CTAGAATGCGAGAGTAGGGAACTGCCGAAGTTCCTATTCTCTAGAAAGTATAGGAACTTCAGCGCTCATGCACTTGATT
CCGGATCCCTAATTAGCGAACGCAGCTGGCTCTCCAA